

10. ELECTROWEAK MODEL AND CONSTRAINTS ON NEW PHYSICS

Revised September 2005 by J. Erler (U. Mexico) and P. Langacker (Univ. of Pennsylvania).

- 10.1 Introduction
- 10.2 Renormalization and radiative corrections
- 10.3 Cross-section and asymmetry formulae
- 10.4 Precision flavor physics
- 10.5 W and Z decays
- 10.6 Experimental results
- 10.7 Constraints on new physics

10.1. Introduction

The standard electroweak model (SM) is based on the gauge group [1] $SU(2) \times U(1)$, with gauge bosons W_μ^i , $i = 1, 2, 3$, and B_μ for the $SU(2)$ and $U(1)$ factors, respectively, and the corresponding gauge coupling constants g and g' . The left-handed fermion fields $\psi_i = \begin{pmatrix} \nu_i \\ \ell_i^- \end{pmatrix}$ and $\begin{pmatrix} u_i \\ d_i' \end{pmatrix}$ of the i^{th} fermion family transform as doublets under $SU(2)$, where $d_i' \equiv \sum_j V_{ij} d_j$, and V is the Cabibbo-Kobayashi-Maskawa mixing matrix. (Constraints on V and tests of universality are discussed in Ref. 2 and in the Section on the Cabibbo-Kobayashi-Maskawa mixing matrix. The extension of the formalism to allow an analogous leptonic mixing matrix is discussed in “Neutrino Mass” in the Particle Listings.) The right-handed fields are $SU(2)$ singlets. In the minimal model there are three fermion families and a single complex Higgs doublet $\phi \equiv \begin{pmatrix} \phi^+ \\ \phi^0 \end{pmatrix}$.

After spontaneous symmetry breaking the Lagrangian for the fermion fields is

$$\begin{aligned}
 \mathcal{L}_F = & \sum_i \bar{\psi}_i \left(i \not{\partial} - m_i - \frac{gm_i H}{2M_W} \right) \psi_i \\
 & - \frac{g}{2\sqrt{2}} \sum_i \bar{\psi}_i \gamma^\mu (1 - \gamma^5) (T^+ W_\mu^+ + T^- W_\mu^-) \psi_i \\
 & - e \sum_i q_i \bar{\psi}_i \gamma^\mu \psi_i A_\mu \\
 & - \frac{g}{2 \cos \theta_W} \sum_i \bar{\psi}_i \gamma^\mu (g_V^i - g_A^i \gamma^5) \psi_i Z_\mu .
 \end{aligned} \tag{10.1}$$

$\theta_W \equiv \tan^{-1}(g'/g)$ is the weak angle; $e = g \sin \theta_W$ is the positron electric charge; and $A \equiv B \cos \theta_W + W^3 \sin \theta_W$ is the (massless) photon field. $W^\pm \equiv (W^1 \mp iW^2)/\sqrt{2}$ and $Z \equiv -B \sin \theta_W + W^3 \cos \theta_W$ are the massive charged and neutral weak boson fields, respectively. T^+ and T^- are the weak isospin raising and lowering operators. The vector

2 10. Electroweak model and constraints on new physics

and axial-vector couplings are

$$g_V^i \equiv t_{3L}(i) - 2q_i \sin^2 \theta_W , \quad (10.2a)$$

$$g_A^i \equiv t_{3L}(i) , \quad (10.2b)$$

where $t_{3L}(i)$ is the weak isospin of fermion i ($+1/2$ for u_i and ν_i ; $-1/2$ for d_i and e_i) and q_i is the charge of ψ_i in units of e .

The second term in \mathcal{L}_F represents the charged-current weak interaction [3,4]. For example, the coupling of a W to an electron and a neutrino is

$$-\frac{e}{2\sqrt{2}\sin\theta_W} \left[W_\mu^- \bar{e} \gamma^\mu (1 - \gamma^5) \nu + W_\mu^+ \bar{\nu} \gamma^\mu (1 - \gamma^5) e \right] . \quad (10.3)$$

For momenta small compared to M_W , this term gives rise to the effective four-fermion interaction with the Fermi constant given (at tree level, *i.e.*, lowest order in perturbation theory) by $G_F/\sqrt{2} = g^2/8M_W^2$. CP violation is incorporated in the SM by a single observable phase in V_{ij} . The third term in \mathcal{L}_F describes electromagnetic interactions (QED), and the last is the weak neutral-current interaction.

In Eq. (10.1), m_i is the mass of the i^{th} fermion ψ_i . For the quarks these are the current masses. For the light quarks, as described in “The Note on Quark Masses” in the Particle Listings, $\hat{m}_u \approx 1.5\text{--}4$ MeV, $\hat{m}_d \approx 4\text{--}8$ MeV, and $\hat{m}_s \approx 80\text{--}130$ MeV. These are running $\overline{\text{MS}}$ masses evaluated at the scale $\mu = 2$ GeV. (In this Section we denote quantities defined in the $\overline{\text{MS}}$ scheme by a caret; the exception is the strong coupling constant, α_s , which will always correspond to the $\overline{\text{MS}}$ definition and where the caret will be dropped.) For the heavier quarks we use QCD sum rule constraints [5] and recalculate their masses in each call of our fits to account for their direct α_s dependence. We find, $\hat{m}_c(\mu = \hat{m}_c) = 1.290_{-0.045}^{+0.040}$ GeV and $\hat{m}_b(\mu = \hat{m}_b) = 4.207 \pm 0.031$ GeV, with a correlation of 29%. The top quark “pole” mass, $m_t = 172.7 \pm 2.9$ GeV, is an average [6] of published CDF [7] and DØ [8] results from run I and of preliminary results from run II. We are working, however, with $\overline{\text{MS}}$ masses in all expressions to minimize theoretical uncertainties, and therefore convert this result to the top quark $\overline{\text{MS}}$ mass,

$$\hat{m}_t(\mu = \hat{m}_t) = m_t \left[1 - \frac{4}{3} \frac{\alpha_s}{\pi} + \mathcal{O}(\alpha_s^2) \right],$$

using the three-loop formula from Ref. 9. This introduces an additional uncertainty which we estimate to 0.6 GeV (the size of the three-loop term). We are assuming that the kinematic mass extracted from the collider events corresponds within this uncertainty to the pole mass. Using the BLM optimized [10] version of the two-loop perturbative QCD formula [11] (as we did in previous editions of this *Review*) gives virtually identical results. Thus, we will use $m_t = 172.7 \pm 2.9 \pm 0.6$ GeV $\approx 172.7 \pm 3.0$ GeV (together with $M_H = 117$ GeV) for the numerical values quoted in Sec. 10.2–Sec. 10.4. In the presence of right-handed neutrinos, Eq. (10.1) gives rise also to Dirac neutrino masses. The possibility of Majorana masses is discussed in “Neutrino mass” in the Particle Listings.

H is the physical neutral Higgs scalar which is the only remaining part of ϕ after spontaneous symmetry breaking. The Yukawa coupling of H to ψ_i , which is flavor diagonal in the minimal model, is $gm_i/2M_W$. In non-minimal models there are additional charged and neutral scalar Higgs particles [12].

10.2. Renormalization and radiative corrections

The SM has three parameters (not counting the Higgs boson mass, M_H , and the fermion masses and mixings). A particularly useful set is:

- (a) The fine structure constant $\alpha = 1/137.03599911(46)$, determined from the e^\pm anomalous magnetic moment, the quantum Hall effect, and other measurements [13]. In most electroweak renormalization schemes, it is convenient to define a running α dependent on the energy scale of the process, with $\alpha^{-1} \sim 137$ appropriate at very low energy. (The running has also been observed directly [14].) For scales above a few hundred MeV this introduces an uncertainty due to the low-energy hadronic contribution to vacuum polarization. In the modified minimal subtraction ($\overline{\text{MS}}$) scheme [15] (used for this *Review*), and with $\alpha_s(M_Z) = 0.120$ for the QCD coupling at M_Z , we have $\hat{\alpha}(m_\tau)^{-1} = 133.445 \pm 0.017$ and $\hat{\alpha}(M_Z)^{-1} = 127.918 \pm 0.018$. The latter corresponds to a quark sector contribution (without the top) to the conventional (on-shell) QED coupling, $\alpha(M_Z) = \frac{\alpha}{1 - \Delta\alpha(M_Z)}$, of $\Delta\alpha_{\text{had}}^{(5)}(M_Z) \approx 0.02791 \pm 0.00013$. These values are updated from Ref. 16 with a reduced uncertainty by a factor of 1/3 because they account for the latest results from τ decays (moving $\Delta\alpha_{\text{had}}^{(5)}(M_Z)$ up by somewhat less than one standard deviation) and a reanalysis of the CMD 2 collaboration results after correcting a radiative correction [17]. See Ref. 18 for a discussion in the context of the anomalous magnetic moment of the muon. The correlation of the latter with $\hat{\alpha}(M_Z)$, as well as the non-linear α_s dependence of $\hat{\alpha}(M_Z)$ and the resulting correlation with the input variable α_s , are fully taken into account in the fits. This is done by using as actual input (fit constraint) instead of $\Delta\alpha_{\text{had}}^{(5)}(M_Z)$ the analogous low-energy contribution by the three light quarks, $\Delta\alpha_{\text{had}}^{(3)}(1.8 \text{ GeV}) = 0.00577 \pm 0.00010$, and by calculating the perturbative and heavy quark contributions to $\hat{\alpha}(M_Z)$ in each call of the fits according to Ref. 16. The uncertainty is from e^+e^- annihilation data below 1.8 GeV and τ decay data, from isospin breaking effects (affecting the interpretation of the τ data); from uncalculated higher order perturbative and non-perturbative QCD corrections; and from the $\overline{\text{MS}}$ quark masses. Such a short distance mass definition (unlike the pole mass) is free from non-perturbative and renormalon uncertainties. Various recent evaluations of $\Delta\alpha_{\text{had}}^{(5)}$ are summarized in Table 10.1, where the relation between the on-shell and $\overline{\text{MS}}$ definitions is given by

$$\Delta\hat{\alpha}(M_Z) - \Delta\alpha(M_Z) = \frac{\alpha}{\pi} \left(\frac{100}{27} - \frac{1}{6} - \frac{7}{4} \ln \frac{M_Z^2}{M_W^2} \right) \approx 0.0072$$

to leading order, where the first term is from fermions and the other two are from W^\pm loops which are usually excluded from the on-shell definition. Most of the older results relied on $e^+e^- \rightarrow \text{hadrons}$ cross-section measurements up to energies of 40 GeV, which were somewhat higher than the QCD prediction, suggested stronger running, and were less precise. The most recent results typically assume the validity of perturbative QCD (PQCD) at scales of 1.8 GeV and above, and are

4 10. Electroweak model and constraints on new physics

in reasonable agreement with each other. (Evaluations in the on-shell scheme utilize resonance data from BES [38] as further input.) There is, however, some discrepancy between analyzes based on $e^+e^- \rightarrow$ hadrons cross-section data and those based on τ decay spectral functions [18–20]. The latter imply lower central values for the extracted M_H of $\mathcal{O}(10 \text{ GeV})$. The discrepancy originates from the kinematic region $\sqrt{s} \gtrsim 0.6 \text{ GeV}$. However, at least some of it appears to be experimental. The $e^+e^- \rightarrow \pi^+\pi^-$ cross-sections measured by the SND collaboration [39] are significantly larger than the older results by the CMD collaboration [40]. The data from SND are also about one standard deviation higher than those by CMD 2 [17] but in perfect agreement with information from τ decays. As an alternative to cross-section scans, one can use the high statistics radiative return events [41] at e^+e^- accelerators operating at resonances such as the Φ or the $\Upsilon(4S)$. The method is systematics dominated. The $\pi^+\pi^-$ radiative return results from the Φ obtained by the KLOE collaboration [42] for energies above the ρ peak are significantly lower compared to SND, while CMD 2 lies in between. Results for three and four pion final states are in better agreement. Further improvement of this dominant theoretical uncertainty in the interpretation of precision data will require better measurements of the cross-section for $e^+e^- \rightarrow$ hadrons below the charmonium resonances, as well as in the threshold region of the heavy quarks (to improve the precision in $\hat{m}_c(\hat{m}_c)$ and $\hat{m}_b(\hat{m}_b)$).

- (b) The Fermi constant, $G_F = 1.16637(1) \times 10^{-5} \text{ GeV}^{-2}$, determined from the muon lifetime formula [43,44],

$$\begin{aligned} \tau_\mu^{-1} &= \frac{G_F^2 m_\mu^5}{192\pi^3} F\left(\frac{m_e^2}{m_\mu^2}\right) \left(1 + \frac{3}{5} \frac{m_\mu^2}{M_W^2}\right) \\ &\times \left[1 + \left(\frac{25}{8} - \frac{\pi^2}{2}\right) \frac{\alpha(m_\mu)}{\pi} + C_2 \frac{\alpha^2(m_\mu)}{\pi^2}\right], \end{aligned} \quad (10.4a)$$

where

$$F(x) = 1 - 8x + 8x^3 - x^4 - 12x^2 \ln x, \quad (10.4b)$$

$$C_2 = \frac{156815}{5184} - \frac{518}{81}\pi^2 - \frac{895}{36}\zeta(3) + \frac{67}{720}\pi^4 + \frac{53}{6}\pi^2 \ln(2), \quad (10.4c)$$

and

$$\alpha(m_\mu)^{-1} = \alpha^{-1} - \frac{2}{3\pi} \ln\left(\frac{m_\mu}{m_e}\right) + \frac{1}{6\pi} \approx 136. \quad (10.4d)$$

The $\mathcal{O}(\alpha^2)$ corrections to μ decay have been completed in Ref. 44. The remaining uncertainty in G_F is from the experimental input.

- (c) The Z -boson mass, $M_Z = 91.1876 \pm 0.0021 \text{ GeV}$, determined from the Z -lineshape scan at LEP 1 [45].

Table 10.1: Recent evaluations of the on-shell $\Delta\alpha_{\text{had}}^{(5)}(M_Z)$. For better comparison we adjusted central values and errors to correspond to a common and fixed value of $\alpha_s(M_Z) = 0.120$. References quoting results without the top quark decoupled are converted to the five flavor definition. Ref. [31] uses $\Lambda_{\text{QCD}} = 380 \pm 60$ MeV; for the conversion we assumed $\alpha_s(M_Z) = 0.118 \pm 0.003$.

Reference	Result	Comment
Martin, Zeppenfeld [21]	0.02744 ± 0.00036	PQCD for $\sqrt{s} > 3$ GeV
Eidelman, Jegerlehner [22]	0.02803 ± 0.00065	PQCD for $\sqrt{s} > 40$ GeV
Geshkenbein, Morgunov [23]	0.02780 ± 0.00006	$\mathcal{O}(\alpha_s)$ resonance model
Burkhardt, Pietrzyk [24]	0.0280 ± 0.0007	PQCD for $\sqrt{s} > 40$ GeV
Swartz [25]	0.02754 ± 0.00046	use of fitting function
Aleman <i>et al.</i> [26]	0.02816 ± 0.00062	incl. τ decay data
Krasnikov, Rodenberg [27]	0.02737 ± 0.00039	PQCD for $\sqrt{s} > 2.3$ GeV
Davier & Höcker [28]	0.02784 ± 0.00022	PQCD for $\sqrt{s} > 1.8$ GeV
Kühn & Steinhauser [29]	0.02778 ± 0.00016	complete $\mathcal{O}(\alpha_s^2)$
Erlar [16]	0.02779 ± 0.00020	conv. from $\overline{\text{MS}}$ scheme
Davier & Höcker [30]	0.02770 ± 0.00015	use of QCD sum rules
Groote <i>et al.</i> [31]	0.02787 ± 0.00032	use of QCD sum rules
Martin <i>et al.</i> [32]	0.02741 ± 0.00019	includes new BES data
Burkhardt, Pietrzyk [33]	0.02763 ± 0.00036	PQCD for $\sqrt{s} > 12$ GeV
de Troconiz, Yndurain [34]	0.02754 ± 0.00010	PQCD for $s > 2$ GeV ²
Jegerlehner [35]	0.02765 ± 0.00013	conv. from MOM scheme
Hagiwara <i>et al.</i> [36]	0.02757 ± 0.00023	PQCD for $\sqrt{s} > 11.09$ GeV
Burkhardt, Pietrzyk [37]	0.02760 ± 0.00035	incl. KLOE data

With these inputs, $\sin^2 \theta_W$ and the W -boson mass, M_W , can be calculated when values for m_t and M_H are given; conversely (as is done at present), M_H can be constrained by $\sin^2 \theta_W$ and M_W . The value of $\sin^2 \theta_W$ is extracted from Z -pole observables and neutral-current processes [45–48], and depends on the renormalization prescription. There are a number of popular schemes [49–56] leading to values which differ by small factors depending on m_t and M_H . The notation for these schemes is shown in Table 10.2. Discussion of the schemes follows the table.

- (i) The on-shell scheme [49] promotes the tree-level formula $\sin^2 \theta_W = 1 - M_W^2/M_Z^2$ to a definition of the renormalized $\sin^2 \theta_W$ to all orders in perturbation theory, *i.e.*,

6 10. Electroweak model and constraints on new physics

Table 10.2: Notations used to indicate the various schemes discussed in the text. Each definition of $\sin\theta_W$ leads to values that differ by small factors depending on m_t and M_H . Approximate values are also given for illustration.

Scheme	Notation and Value
On-shell	$(s_W)^2 = \sin^2\theta_W \approx 0.2231$
NOV	$(s_{M_Z})^2 = \sin^2\theta_W \approx 0.2311$
$\overline{\text{MS}}$	$(\widehat{s}_Z)^2 = \sin^2\theta_W \approx 0.2312$
$\overline{\text{MS}}$ ND	$(\widehat{s}_{\text{ND}})^2 = \sin^2\theta_W \approx 0.2314$
Effective angle	$(\overline{s}_f)^2 = \sin^2\theta_W \approx 0.2315$

$\sin^2\theta_W \rightarrow s_W^2 \equiv 1 - M_W^2/M_Z^2$:

$$M_W = \frac{A_0}{s_W(1 - \Delta r)^{1/2}}, \quad (10.5a)$$

$$M_Z = \frac{M_W}{c_W}, \quad (10.5b)$$

where $c_W \equiv \cos\theta_W$, $A_0 = (\pi\alpha/\sqrt{2}G_F)^{1/2} = 37.2805(2)$ GeV, and Δr includes the radiative corrections relating α , $\alpha(M_Z)$, G_F , M_W , and M_Z . One finds $\Delta r \sim \Delta r_0 - \rho_t/\tan^2\theta_W$, where $\Delta r_0 = 1 - \alpha/\widehat{\alpha}(M_Z) = 0.06654(14)$ is due to the running of α , and $\rho_t = 3G_F m_t^2/8\sqrt{2}\pi^2 = 0.00935(m_t/172.7 \text{ GeV})^2$ represents the dominant (quadratic) m_t dependence. There are additional contributions to Δr from bosonic loops, including those which depend logarithmically on M_H . One has $\Delta r = 0.03630 \mp 0.0011 \pm 0.00014$, where the second uncertainty is from $\alpha(M_Z)$. Thus the value of s_W^2 extracted from M_Z includes an uncertainty (∓ 0.00036) from the currently allowed range of m_t . This scheme is simple conceptually. However, the relatively large ($\sim 3\%$) correction from ρ_t causes large spurious contributions in higher orders.

- (ii) A more precisely determined quantity $s_{M_Z}^2$ [50] can be obtained from M_Z by removing the (m_t, M_H) dependent term from Δr [51], *i.e.*,

$$s_{M_Z}^2 c_{M_Z}^2 \equiv \frac{\pi\alpha(M_Z)}{\sqrt{2}G_F M_Z^2}. \quad (10.6)$$

Using $\alpha(M_Z)^{-1} = 128.91 \pm 0.02$ yields $s_{M_Z}^2 = 0.23108 \mp 0.00005$. The small uncertainty in $s_{M_Z}^2$ compared to other schemes is because most of the m_t dependence has been removed by definition. However, the m_t uncertainty reemerges when other quantities (*e.g.*, M_W or other Z -pole observables) are predicted in terms of M_Z .

10. Electroweak model and constraints on new physics 7

Both s_W^2 and $s_{M_Z}^2$ depend not only on the gauge couplings but also on the spontaneous-symmetry breaking, and both definitions are awkward in the presence of any extension of the SM which perturbs the value of M_Z (or M_W). Other definitions are motivated by the tree-level coupling constant definition $\theta_W = \tan^{-1}(g'/g)$.

- (iii) In particular, the modified minimal subtraction ($\overline{\text{MS}}$) scheme introduces the quantity $\sin^2 \hat{\theta}_W(\mu) \equiv \hat{g}'^2(\mu)/[\hat{g}^2(\mu) + \hat{g}'^2(\mu)]$, where the couplings \hat{g} and \hat{g}' are defined by modified minimal subtraction and the scale μ is conveniently chosen to be M_Z for many electroweak processes. The value of $\hat{s}_Z^2 = \sin^2 \hat{\theta}_W(M_Z)$ extracted from M_Z is less sensitive than s_W^2 to m_t (by a factor of $\tan^2 \theta_W$), and is less sensitive to most types of new physics than s_W^2 or $s_{M_Z}^2$. It is also very useful for comparing with the predictions of grand unification. There are actually several variant definitions of $\sin^2 \hat{\theta}_W(M_Z)$, differing according to whether or how finite $\alpha \ln(m_t/M_Z)$ terms are decoupled (subtracted from the couplings). One cannot entirely decouple the $\alpha \ln(m_t/M_Z)$ terms from all electroweak quantities because $m_t \gg m_b$ breaks SU(2) symmetry. The scheme that will be adopted here decouples the $\alpha \ln(m_t/M_Z)$ terms from the γ - Z mixing [15,52], essentially eliminating any $\ln(m_t/M_Z)$ dependence in the formulae for asymmetries at the Z -pole when written in terms of \hat{s}_Z^2 . (A similar definition is used for $\hat{\alpha}$.) The various definitions are related by

$$\hat{s}_Z^2 = c(m_t, M_H) s_W^2 = \bar{c}(m_t, M_H) s_{M_Z}^2, \quad (10.7)$$

where $c = 1.0359 \pm 0.0012$ and $\bar{c} = 1.0010 \mp 0.0004$. The quadratic m_t dependence is given by $c \sim 1 + \rho_t/\tan^2 \theta_W$ and $\bar{c} \sim 1 - \rho_t/(1 - \tan^2 \theta_W)$, respectively. The expressions for M_W and M_Z in the $\overline{\text{MS}}$ scheme are

$$M_W = \frac{A_0}{\hat{s}_Z(1 - \Delta \hat{r}_W)^{1/2}}, \quad (10.8a)$$

$$M_Z = \frac{M_W}{\hat{\rho}^{1/2} \hat{c}_Z}, \quad (10.8b)$$

and one predicts $\Delta \hat{r}_W = 0.06969 \pm 0.00004 \pm 0.00014$. $\Delta \hat{r}_W$ has no quadratic m_t dependence, because shifts in M_W are absorbed into the observed G_F , so that the error in $\Delta \hat{r}_W$ is dominated by $\Delta r_0 = 1 - \alpha/\hat{\alpha}(M_Z)$ which induces the second quoted uncertainty. The quadratic m_t dependence has been shifted into $\hat{\rho} \sim 1 + \rho_t$, where including bosonic loops, $\hat{\rho} = 1.01043 \pm 0.00034$. Quadratic M_H effects are deferred to two-loop order, while the leading logarithmic M_H effects are dominant only for large M_H values which are currently disfavored by the precision data. As an illustration, the shift in M_W due to a large M_H (for fixed M_Z) is given by

$$\Delta_H M_W = -\frac{11}{96} \frac{\alpha}{\pi} \frac{M_W}{c_W^2 - s_W^2} \ln \frac{M_H^2}{M_W^2} + \mathcal{O}(\alpha^2). \quad (10.9)$$

- (iv) A variant $\overline{\text{MS}}$ quantity \hat{s}_{ND}^2 (used in the 1992 edition of this *Review*) does not decouple the $\alpha \ln(m_t/M_Z)$ terms [53]. It is related to \hat{s}_Z^2 by

$$\hat{s}_Z^2 = \hat{s}_{\text{ND}}^2 / \left(1 + \frac{\hat{\alpha}}{\pi} d\right), \quad (10.10a)$$

8 10. Electroweak model and constraints on new physics

$$d = \frac{1}{3} \left(\frac{1}{\widehat{s}^2} - \frac{8}{3} \right) \left[\left(1 + \frac{\alpha_s}{\pi} \right) \ln \frac{m_t}{M_Z} - \frac{15\alpha_s}{8\pi} \right], \quad (10.10b)$$

Thus, $\widehat{s}_Z^2 - \widehat{s}_{\text{ND}}^2 \sim -0.0002$ for $m_t = 172.7$ GeV.

- (v) Yet another definition, the effective angle [54–56] \overline{s}_f^2 for the Z vector coupling to fermion f , is described in Sec. 10.3.

Experiments are at a level of precision that complete $\mathcal{O}(\alpha)$ radiative corrections must be applied. For neutral-current and Z -pole processes, these corrections are conveniently divided into two classes:

1. QED diagrams involving the emission of real photons or the exchange of virtual photons in loops, but not including vacuum polarization diagrams. These graphs often yield finite and gauge-invariant contributions to observable processes. However, they are dependent on energies, experimental cuts, *etc.*, and must be calculated individually for each experiment.
2. Electroweak corrections, including $\gamma\gamma$, γZ , ZZ , and WW vacuum polarization diagrams, as well as vertex corrections, box graphs, *etc.*, involving virtual W 's and Z 's. Many of these corrections are absorbed into the renormalized Fermi constant defined in Eq. (10.4). Others modify the tree-level expressions for Z -pole observables and neutral-current amplitudes in several ways [46]. One-loop corrections are included for all processes. In addition, certain two-loop corrections are also important. In particular, two-loop corrections involving the top quark modify ρ_t in $\widehat{\rho}$, Δr , and elsewhere by

$$\rho_t \rightarrow \rho_t [1 + R(M_H, m_t) \rho_t / 3]. \quad (10.11)$$

$R(M_H, m_t)$ is best described as an expansion in M_Z^2/m_t^2 . The unsuppressed terms were first obtained in Ref. 57, and are known analytically [58]. Contributions suppressed by M_Z^2/m_t^2 were first studied in Ref. 59 with the help of small and large Higgs mass expansions, which can be interpolated. These contributions are about as large as the leading ones in Refs. 57 and 58. The complete two-loop calculation of Δr (without further approximation) has been performed in Refs. 60,61 for fermionic and purely bosonic diagrams, respectively. Similarly, the electroweak two-loop calculation for the relation between \overline{s}_ℓ^2 and s_W^2 is complete [62] except for the purely bosonic contribution. For M_H above its lower direct limit, $-17 < R \leq -13$.

Mixed QCD-electroweak contributions to gauge boson self-energies of order $\alpha\alpha_s m_t^2$ [63] and $\alpha\alpha_s^2 m_t^2$ [64] increase the predicted value of m_t by 6%. This is, however, almost entirely an artifact of using the pole mass definition for m_t . The equivalent corrections when using the $\overline{\text{MS}}$ definition $\widehat{m}_t(\widehat{m}_t)$ increase m_t by less than 0.5%. The subleading $\alpha\alpha_s$ corrections [65] are also included. Further three-loop corrections of order $\alpha\alpha_s^2$ [66], $\alpha^3 m_t^6$ [67,68], and $\alpha^2 \alpha_s m_t^4$ (for $M_H = 0$) [67], are rather small. The same is true for $\alpha^3 M_H^4$ [69] corrections unless M_H approaches 1 TeV.

The leading electroweak two-loop terms for the $Z \rightarrow b\bar{b}$ -vertex of $\mathcal{O}(\alpha^2 m_t^4)$ have been obtained in Refs. 57,58, and the mixed QCD-electroweak contributions

in Refs. 70,71. The $\mathcal{O}(\alpha\alpha_s)$ -vertex corrections involving massless quarks [72] add coherently, resulting in a sizable effect and shift the extracted $\alpha_s(M_Z)$ by $\approx +0.0007$.

Throughout this *Review* we utilize electroweak radiative corrections from the program GAPP [73], which works entirely in the $\overline{\text{MS}}$ scheme, and which is independent of the package ZFITTER [56].

10.3. Cross-section and asymmetry formulae

It is convenient to write the four-fermion interactions relevant to ν -hadron, ν - e , and parity violating e -hadron neutral-current processes in a form that is valid in an arbitrary gauge theory (assuming massless left-handed neutrinos). One has

$$-\mathcal{L}^{\nu\text{Hadron}} = \frac{G_F}{\sqrt{2}} \bar{\nu} \gamma^\mu (1 - \gamma^5) \nu$$

$$\times \sum_i \left[\epsilon_L(i) \bar{q}_i \gamma_\mu (1 - \gamma^5) q_i + \epsilon_R(i) \bar{q}_i \gamma_\mu (1 + \gamma^5) q_i \right], \quad (10.12)$$

$$-\mathcal{L}^{\nu e} = \frac{G_F}{\sqrt{2}} \bar{\nu}_\mu \gamma^\mu (1 - \gamma^5) \nu_\mu \bar{e} \gamma_\mu (g_V^{\nu e} - g_A^{\nu e} \gamma^5) e \quad (10.13)$$

(for ν_e - e or $\bar{\nu}_e$ - e , the charged-current contribution must be included), and

$$-\mathcal{L}^{e\text{Hadron}} = -\frac{G_F}{\sqrt{2}}$$

$$\times \sum_i \left[C_{1i} \bar{e} \gamma_\mu \gamma^5 e \bar{q}_i \gamma^\mu q_i + C_{2i} \bar{e} \gamma_\mu e \bar{q}_i \gamma^\mu \gamma^5 q_i \right]. \quad (10.14)$$

(One must add the parity-conserving QED contribution.)

The SM expressions for $\epsilon_{L,R}(i)$, $g_{V,A}^{\nu e}$, and C_{ij} are given in Table 10.3. Note, that $g_{V,A}^{\nu e}$ and the other quantities are coefficients of effective four-Fermi operators, which differ from the quantities defined in Eq. (10.2) in the radiative corrections and in the presence of possible physics beyond the SM.

A precise determination of the on-shell s_W^2 , which depends only very weakly on m_t and M_H , is obtained from deep inelastic neutrino scattering from (approximately) isoscalar targets [74]. The ratio $R_\nu \equiv \sigma_{\nu N}^{NC} / \sigma_{\nu N}^{CC}$ of neutral- to charged-current cross-sections has been measured to 1% accuracy by the CDHS [75] and CHARM [76] collaborations at CERN. The CCFR [77] collaboration at Fermilab has obtained an even more precise result and the NOMAD [78] collaboration anticipates a 0.3% measurement, so it is important to obtain theoretical expressions for R_ν and $R_{\bar{\nu}} \equiv \sigma_{\bar{\nu} N}^{NC} / \sigma_{\bar{\nu} N}^{CC}$ to comparable accuracy. Fortunately, most of the uncertainties from the strong interactions and neutrino spectra cancel in the ratio. The largest theoretical uncertainty is associated with the c -threshold, which mainly affects σ^{CC} . Using the slow rescaling prescription [79] the central value of $\sin^2 \theta_W$ from CCFR varies as $0.0111(m_c [\text{GeV}] - 1.31)$, where m_c is the effective

10 10. Electroweak model and constraints on new physics

Table 10.3: Standard Model expressions for the neutral-current parameters for ν -hadron, ν - e , and e -hadron processes. At tree level, $\rho = \kappa = 1$, $\lambda = 0$. If radiative corrections are included, $\rho_{\nu N}^{NC} = 1.0081$, $\widehat{\kappa}_{\nu N}(\langle Q^2 \rangle = -12 \text{ GeV}^2) = 0.9978$, $\widehat{\kappa}_{\nu N}(\langle Q^2 \rangle = -35 \text{ GeV}^2) = 0.9964$, $\lambda_{uL} = -0.0031$, $\lambda_{dL} = -0.0025$, and $\lambda_{dR} = 2 \lambda_{uR} = 7.5 \times 10^{-5}$. For ν - e scattering, $\rho_{\nu e} = 1.0127$ and $\widehat{\kappa}_{\nu e} = 0.9965$ (at $\langle Q^2 \rangle = 0$). For atomic parity violation and the SLAC polarized electron experiment, $\rho'_{eq} = 0.9876$, $\rho_{eq} = 1.0006$, $\widehat{\kappa}'_{eq} = 1.0026$, $\widehat{\kappa}_{eq} = 1.0299$, $\lambda_{1d} = -2 \lambda_{1u} = 3.6 \times 10^{-5}$, $\lambda_{2u} = -0.0121$ and $\lambda_{2d} = 0.0026$. The dominant m_t dependence is given by $\rho \sim 1 + \rho_t$, while $\widehat{\kappa} \sim 1$ ($\overline{\text{MS}}$) or $\kappa \sim 1 + \rho_t / \tan^2 \theta_W$ (on-shell).

Quantity	Standard Model Expression
$\epsilon_L(u)$	$\rho_{\nu N}^{NC} \left(\frac{1}{2} - \frac{2}{3} \widehat{\kappa}_{\nu N} \widehat{s}_Z^2 \right) + \lambda_{uL}$
$\epsilon_L(d)$	$\rho_{\nu N}^{NC} \left(-\frac{1}{2} + \frac{1}{3} \widehat{\kappa}_{\nu N} \widehat{s}_Z^2 \right) + \lambda_{dL}$
$\epsilon_R(u)$	$\rho_{\nu N}^{NC} \left(-\frac{2}{3} \widehat{\kappa}_{\nu N} \widehat{s}_Z^2 \right) + \lambda_{uR}$
$\epsilon_R(d)$	$\rho_{\nu N}^{NC} \left(\frac{1}{3} \widehat{\kappa}_{\nu N} \widehat{s}_Z^2 \right) + \lambda_{dR}$
$g_V^{\nu e}$	$\rho_{\nu e} \left(-\frac{1}{2} + 2 \widehat{\kappa}_{\nu e} \widehat{s}_Z^2 \right)$
$g_A^{\nu e}$	$\rho_{\nu e} \left(-\frac{1}{2} \right)$
C_{1u}	$\rho'_{eq} \left(-\frac{1}{2} + \frac{4}{3} \widehat{\kappa}'_{eq} \widehat{s}_Z^2 \right) + \lambda_{1u}$
C_{1d}	$\rho'_{eq} \left(\frac{1}{2} - \frac{2}{3} \widehat{\kappa}'_{eq} \widehat{s}_Z^2 \right) + \lambda_{1d}$
C_{2u}	$\rho_{eq} \left(-\frac{1}{2} + 2 \widehat{\kappa}_{eq} \widehat{s}_Z^2 \right) + \lambda_{2u}$
C_{2d}	$\rho_{eq} \left(\frac{1}{2} - 2 \widehat{\kappa}_{eq} \widehat{s}_Z^2 \right) + \lambda_{2d}$

mass which is numerically close to the $\overline{\text{MS}}$ mass $\widehat{m}_c(\widehat{m}_c)$, but their exact relation is unknown at higher orders. For $m_c = 1.31 \pm 0.24 \text{ GeV}$ (determined from ν -induced dimuon production [80]) this contributes ± 0.003 to the total uncertainty $\Delta \sin^2 \theta_W \sim \pm 0.004$. (The experimental uncertainty is also ± 0.003 .) This uncertainty largely cancels, however, in the Paschos-Wolfenstein ratio [81],

$$R^- = \frac{\sigma_{\nu N}^{NC} - \sigma_{\bar{\nu} N}^{NC}}{\sigma_{\nu N}^{CC} - \sigma_{\bar{\nu} N}^{CC}}. \quad (10.15)$$

It was measured by the NuTeV collaboration [82] for the first time, and required a high-intensity and high-energy anti-neutrino beam.

A simple zeroth-order approximation is

$$R_\nu = g_L^2 + g_R^2 r , \quad (10.16a)$$

$$R_{\bar{\nu}} = g_L^2 + \frac{g_R^2}{r} , \quad (10.16b)$$

$$R^- = g_L^2 - g_R^2 , \quad (10.16c)$$

where

$$g_L^2 \equiv \epsilon_L(u)^2 + \epsilon_L(d)^2 \approx \frac{1}{2} - \sin^2 \theta_W + \frac{5}{9} \sin^4 \theta_W , \quad (10.17a)$$

$$g_R^2 \equiv \epsilon_R(u)^2 + \epsilon_R(d)^2 \approx \frac{5}{9} \sin^4 \theta_W , \quad (10.17b)$$

and $r \equiv \sigma_{\bar{\nu}N}^{CC}/\sigma_{\nu N}^{CC}$ is the ratio of $\bar{\nu}$ and ν charged-current cross-sections, which can be measured directly. (In the simple parton model, ignoring hadron energy cuts, $r \approx (\frac{1}{3} + \epsilon)/(1 + \frac{1}{3}\epsilon)$, where $\epsilon \sim 0.125$ is the ratio of the fraction of the nucleon's momentum carried by anti-quarks to that carried by quarks.) In practice, Eq. (10.16) must be corrected for quark mixing, quark sea effects, c -quark threshold effects, non-isoscalarity, W - Z propagator differences, the finite muon mass, QED and electroweak radiative corrections. Details of the neutrino spectra, experimental cuts, x and Q^2 dependence of structure functions, and longitudinal structure functions enter only at the level of these corrections and therefore lead to very small uncertainties. The CCFR group quotes $s_W^2 = 0.2236 \pm 0.0041$ for $(m_t, M_H) = (175, 150)$ GeV with very little sensitivity to (m_t, M_H) .

The NuTeV collaboration finds $s_W^2 = 0.2277 \pm 0.0016$ (for the same reference values) which is 3.0σ higher than the SM prediction. The discrepancy is in the left-handed coupling, $g_L^2 = 0.3000 \pm 0.0014$, which is 2.7σ low, while $g_R^2 = 0.0308 \pm 0.0011$ is 0.6σ high. Within the SM, we can identify four categories of effects that could cause or contribute to this effect [83]. (i) An asymmetric strange sea [84] by itself is an unlikely explanation, but if this asymmetry takes a positive value it would reduce the discrepancy. A preliminary analysis of dimuon data [85] in the relevant kinematic regime, however, indicates a negative strange asymmetry [86]. On the other hand, Ref. 87 finds the opposite sign, at least in its best fit solution. The two analyzes are not directly comparable, however, since the NuTeV Collaboration [85] used a next-to-leading order fit, but with only a subset of the data. In addition, NuTeV does not constrain its parton distribution functions (PDFs) to yield vanishing net strangeness for the proton. Ref. 87 is a leading-order fit to world data including the net strangeness constraint. (ii) Another possibility is that the PDFs violate isospin symmetry at levels much stronger than generally expected [88]. A minimum χ^2 set of PDFs generalized in this sense [89] shows a reduction in the NuTeV discrepancy in s_W^2 by 0.0015. But isospin symmetry violating PDFs are currently not well constrained and within uncertainties the NuTeV anomaly could be accounted for in full or conversely made larger [89]. (iii) Nuclear physics effects by themselves appear too small to explain the NuTeV anomaly [90]. In particular, while nuclear shadowing corrections are likely to affect the interpretation of the NuTeV

12 10. Electroweak model and constraints on new physics

result [91] at some level, the NuTeV Collaboration argues that their data are dominated by values of Q^2 at which nuclear shadowing is expected to be relatively small. The model of Ref. 92 indicates that nuclear shadowing effects differ for CC and NC cross-sections as well as ν and $\bar{\nu}$ (both would affect the extraction of s_W^2), but also that $R_{\bar{\nu}}$ is affected more than R_ν , while the anomaly is in the latter. Overall, the model predicts a shift in s_W^2 by about 0.001 with a sign corresponding to a reduction of the discrepancy. (iv) The extracted s_W^2 may also shift at the level of the quoted uncertainty when analyzed using the most recent set of QED and electroweak radiative corrections [93,94], as well as QCD corrections to the structure functions [95]. However, their precise impact can be estimated only after the NuTeV data have been analyzed with a new set of PDFs including these new radiative corrections while simultaneously allowing isospin breaking and asymmetric strange seas. A step in this direction was taken in Ref. 96 in which QED induced isospin violations were shown to reduce the NuTeV discrepancy by 10–20%. Remaining one- and two-loop radiative corrections have been estimated [94] to induce uncertainties in the extracted s_W^2 of ± 0.0004 and ± 0.0003 , respectively. In view of these developments and caveats, we consider the NuTeV result and the other neutrino deep inelastic scattering (DIS) data as preliminary until a re-analysis using PDFs including all experimental and theoretical information has been completed. It is well conceivable that various effects add up to bring the NuTeV result in line with the SM prediction. It is likely that the overall uncertainties in g_L^2 and g_R^2 will increase, but at the same time the older neutrino DIS results may become more precise when analyzed with better PDFs than were available at the time.

The cross-section in the laboratory system for $\nu_\mu e \rightarrow \nu_\mu e$ or $\bar{\nu}_\mu e \rightarrow \bar{\nu}_\mu e$ elastic scattering is

$$\begin{aligned} \frac{d\sigma_{\nu_\mu, \bar{\nu}_\mu}}{dy} &= \frac{G_F^2 m_e E_\nu}{2\pi} \\ &\times \left[(g_V^{\nu e} \pm g_A^{\nu e})^2 + (g_V^{\nu e} \mp g_A^{\nu e})^2 (1-y)^2 \right. \\ &\quad \left. - (g_V^{\nu e 2} - g_A^{\nu e 2}) \frac{y m_e}{E_\nu} \right], \end{aligned} \quad (10.18)$$

where the upper (lower) sign refers to ν_μ ($\bar{\nu}_\mu$), and $y \equiv T_e/E_\nu$ (which runs from 0 to $(1 + m_e/2E_\nu)^{-1}$) is the ratio of the kinetic energy of the recoil electron to the incident ν or $\bar{\nu}$ energy. For $E_\nu \gg m_e$ this yields a total cross-section

$$\sigma = \frac{G_F^2 m_e E_\nu}{2\pi} \left[(g_V^{\nu e} \pm g_A^{\nu e})^2 + \frac{1}{3} (g_V^{\nu e} \mp g_A^{\nu e})^2 \right]. \quad (10.19)$$

The most accurate leptonic measurements [97–100] of $\sin^2 \theta_W$ are from the ratio $R \equiv \sigma_{\nu_\mu e} / \sigma_{\bar{\nu}_\mu e}$ in which many of the systematic uncertainties cancel. Radiative corrections (other than m_t effects) are small compared to the precision of present experiments and have negligible effect on the extracted $\sin^2 \theta_W$. The most precise experiment (CHARM II) [99] determined not only $\sin^2 \theta_W$ but $g_{V,A}^{\nu e}$ as well. The

cross-sections for ν_e - e and $\bar{\nu}_e$ - e may be obtained from Eq. (10.18) by replacing $g_{V,A}^{\nu_e}$ by $g_{V,A}^{\nu_e} + 1$, where the 1 is due to the charged-current contribution [100,101].

The SLAC polarized-electron experiment [102] measured the parity-violating asymmetry

$$A = \frac{\sigma_R - \sigma_L}{\sigma_R + \sigma_L}, \quad (10.20)$$

where $\sigma_{R,L}$ is the cross-section for the deep-inelastic scattering of a right- or left-handed electron: $e_{R,L}N \rightarrow eX$. In the quark parton model

$$\frac{A}{Q^2} = a_1 + a_2 \frac{1 - (1 - y)^2}{1 + (1 - y)^2}, \quad (10.21)$$

where $Q^2 > 0$ is the momentum transfer and y is the fractional energy transfer from the electron to the hadrons. For the deuteron or other isoscalar targets, one has, neglecting the s -quark and anti-quarks,

$$a_1 = \frac{3G_F}{5\sqrt{2}\pi\alpha} \left(C_{1u} - \frac{1}{2}C_{1d} \right) \approx \frac{3G_F}{5\sqrt{2}\pi\alpha} \left(-\frac{3}{4} + \frac{5}{3}\sin^2\theta_W \right), \quad (10.22a)$$

$$a_2 = \frac{3G_F}{5\sqrt{2}\pi\alpha} \left(C_{2u} - \frac{1}{2}C_{2d} \right) \approx \frac{9G_F}{5\sqrt{2}\pi\alpha} \left(\sin^2\theta_W - \frac{1}{4} \right). \quad (10.22b)$$

In another polarized-electron scattering experiment on deuterons, but in the quasi-elastic kinematic regime, the SAMPLE experiment [103] at MIT-Bates extracted the combination $C_{2u} - C_{2d}$ at Q^2 values of 0.1 GeV² and 0.038 GeV². What was actually determined were nucleon form factors from which the quoted results were obtained by the removal of a multi-quark radiative correction. Other linear combinations of the C_{iq} have been determined in polarized-lepton scattering at CERN in μ -C DIS, at Mainz in e -Be (quasi-elastic), and at Bates in e -C (elastic). See the review articles in Refs. [47,102] for more details.

There are now precise experiments measuring atomic parity violation (APV) [104] in cesium [105,106] (at the 0.4% level [105]), thallium [107], lead [108], and bismuth [109]. The uncertainties associated with atomic wave functions are quite small for cesium [110], and have been reduced recently to about 0.4%. In the past, the semi-empirical value of the tensor polarizability added another source of theoretical uncertainty [111]. The ratio of the off-diagonal hyperfine amplitude to the polarizability has now been measured directly by the Boulder group [112]. Combined with the precisely known hyperfine amplitude [113] one finds excellent agreement with the earlier results, reducing the overall theory uncertainty to only 0.5% (while slightly increasing the experimental error). An earlier 2.3 σ deviation from the SM (see the year 2000 edition of this *Review*) is now seen at the 1 σ level, after the contributions from the Breit interaction have been reevaluated [114], and after the subsequent inclusion of other large and previously underestimated effects [115] (*e.g.*, from QED radiative corrections), and an update of the SM calculation [116] resulted in a vanishing net effect. The theoretical uncertainties

14 10. Electroweak model and constraints on new physics

are 3% for thallium [117] but larger for the other atoms. For heavy atoms one determines the “weak charge”

$$Q_W = -2 [C_{1u} (2Z + N) + C_{1d} (Z + 2N)] \approx Z(1 - 4 \sin^2 \theta_W) - N . \quad (10.23)$$

The recent Boulder experiment in cesium also observed the parity-violating weak corrections to the nuclear electromagnetic vertex (the anapole moment [118]) .

In the future it could be possible to reduce the theoretical wave function uncertainties by taking the ratios of parity violation in different isotopes [104,119]. There would still be some residual uncertainties from differences in the neutron charge radii, however [120].

The forward-backward asymmetry for $e^+e^- \rightarrow \ell^+\ell^-$, $\ell = \mu$ or τ , is defined as

$$A_{FB} \equiv \frac{\sigma_F - \sigma_B}{\sigma_F + \sigma_B} , \quad (10.24)$$

where $\sigma_F(\sigma_B)$ is the cross-section for ℓ^- to travel forward (backward) with respect to the e^- direction. A_{FB} and R , the total cross-section relative to pure QED, are given by

$$R = F_1 , \quad (10.25)$$

$$A_{FB} = 3F_2/4F_1 , \quad (10.26)$$

where

$$F_1 = 1 - 2\chi_0 g_V^e g_V^\ell \cos \delta_R + \chi_0^2 (g_V^{e2} + g_A^{e2}) (g_V^{\ell2} + g_A^{\ell2}) , \quad (10.27a)$$

$$F_2 = -2\chi_0 g_A^e g_A^\ell \cos \delta_R + 4\chi_0^2 g_A^e g_A^\ell g_V^e g_V^\ell , \quad (10.27b)$$

$$\tan \delta_R = \frac{M_Z \Gamma_Z}{M_Z^2 - s} , \quad (10.28)$$

$$\chi_0 = \frac{G_F}{2\sqrt{2}\pi\alpha} \frac{sM_Z^2}{[(M_Z^2 - s)^2 + M_Z^2 \Gamma_Z^2]^{1/2}} , \quad (10.29)$$

and \sqrt{s} is the CM energy. Eq. (10.27) is valid at tree level. If the data are radiatively corrected for QED effects (as described above), then the remaining electroweak corrections can be incorporated [121,122] (in an approximation adequate for existing PEP, PETRA, and TRISTAN data, which are well below the Z -pole) by replacing χ_0 by $\chi(s) \equiv (1 + \rho_t)\chi_0(s)\alpha/\alpha(s)$, where $\alpha(s)$ is the running QED coupling, and evaluating g_V in the $\overline{\text{MS}}$ scheme. Reviews and formulae for $e^+e^- \rightarrow \text{hadrons}$ may be found in Ref. 123.

At LEP and SLC, there were high-precision measurements of various Z -pole observables [45,124–130], as summarized in Table 10.5. These include the Z -mass and total width, Γ_Z , and partial widths $\Gamma(f\bar{f})$ for $Z \rightarrow f\bar{f}$ where fermion $f = e, \mu, \tau$, hadrons, b , or c . It is convenient to use the variables $M_Z, \Gamma_Z, R_{\ell_i} \equiv \Gamma(\text{had})/\Gamma(\ell_i^+\ell_i^-)$ ($\ell_i = e, \mu, \tau$), $\sigma_{\text{had}} \equiv 12\pi\Gamma(e^+e^-)\Gamma(\text{had})/M_Z^2 \Gamma_Z^2$, $R_b \equiv \Gamma(b\bar{b})/\Gamma(\text{had})$, and $R_c \equiv \Gamma(c\bar{c})/\Gamma(\text{had})$, most of which are weakly correlated experimentally. ($\Gamma(\text{had})$ is the partial width into hadrons.)

The three values for R_{ℓ_i} are not inconsistent with lepton universality (although R_τ is somewhat low), but we use the general analysis in which the three observables are treated as independent. Similar remarks apply to A_{FB}^{0,ℓ_i} below ($A_{FB}^{0,\tau}$ is somewhat high). $\mathcal{O}(\alpha^3)$ QED corrections introduce a large anti-correlation (-30%) between Γ_Z and σ_{had} . The anti-correlation between R_b and R_c is -18% [45]. The R_{ℓ_i} are insensitive to m_t except for the $Z \rightarrow b\bar{b}$ vertex and final state corrections and the implicit dependence through $\sin^2\theta_W$. Thus, they are especially useful for constraining α_s . The width for invisible decays [45], $\Gamma(\text{inv}) = \Gamma_Z - 3\Gamma(\ell^+\ell^-) - \Gamma(\text{had}) = 499.0 \pm 1.5$ MeV, can be used to determine the number of neutrino flavors much lighter than $M_Z/2$, $N_\nu = \Gamma(\text{inv})/\Gamma^{\text{theory}}(\nu\bar{\nu}) = 2.984 \pm 0.009$ for $(m_t, M_H) = (172.7, 117)$ GeV.

There were also measurements of various Z -pole asymmetries. These include the polarization or left-right asymmetry

$$A_{LR} \equiv \frac{\sigma_L - \sigma_R}{\sigma_L + \sigma_R}, \quad (10.30)$$

where $\sigma_L(\sigma_R)$ is the cross-section for a left-(right-)handed incident electron. A_{LR} was measured precisely by the SLD collaboration at the SLC [125], and has the advantages of being extremely sensitive to $\sin^2\theta_W$ and that systematic uncertainties largely cancel. In addition, the SLD collaboration extracted the final-state couplings A_b, A_c [45], A_s [126], A_τ , and A_μ [127] from left-right forward-backward asymmetries, using

$$A_{LR}^{FB}(f) = \frac{\sigma_{LF}^f - \sigma_{LB}^f - \sigma_{RF}^f + \sigma_{RB}^f}{\sigma_{LF}^f + \sigma_{LB}^f + \sigma_{RF}^f + \sigma_{RB}^f} = \frac{3}{4}A_f, \quad (10.31)$$

where, for example, σ_{LF} is the cross-section for a left-handed incident electron to produce a fermion f traveling in the forward hemisphere. Similarly, A_τ was measured at LEP [45] through the negative total τ polarization, \mathcal{P}_τ , and A_e was extracted from the angular distribution of \mathcal{P}_τ . An equation such as (10.31) assumes that initial state QED corrections, photon exchange, γ - Z interference, the tiny electroweak boxes, and corrections for $\sqrt{s} \neq M_Z$ are removed from the data, leaving the pure electroweak asymmetries. This allows the use of effective tree-level expressions,

$$A_{LR} = A_e P_e, \quad (10.32)$$

$$A_{FB} = \frac{3}{4}A_f \frac{A_e + P_e}{1 + P_e A_e}, \quad (10.33)$$

where

$$A_f \equiv \frac{2\bar{g}_V^f \bar{g}_A^f}{\bar{g}_V^{f2} + \bar{g}_A^{f2}}, \quad (10.34)$$

and

$$\bar{g}_V^f = \sqrt{\rho_f} (t_{3L}^{(f)} - 2q_f \kappa_f \sin^2\theta_W), \quad (10.34b)$$

$$\bar{g}_A^f = \sqrt{\rho_f} t_{3L}^{(f)}. \quad (10.34c)$$

16 10. Electroweak model and constraints on new physics

P_e is the initial e^- polarization, so that the second equality in Eq. (10.31) is reproduced for $P_e = 1$, and the Z -pole forward-backward asymmetries at LEP ($P_e = 0$) are given by $A_{FB}^{(0,f)} = \frac{3}{4}A_e A_f$ where $f = e, \mu, \tau, b, c, s$ [128], and q , and where $A_{FB}^{(0,q)}$ refers to the hadronic charge asymmetry. Corrections for t -channel exchange and s/t -channel interference cause $A_{FB}^{(0,e)}$ to be strongly anti-correlated with R_e (-37%). The correlation between $A_{FB}^{(0,b)}$ and $A_{FB}^{(0,c)}$ amounts to 15%. The initial state coupling, A_e , was also determined through the left-right charge asymmetry [129] and in polarized Bhabba scattering at the SLC [127]. The forward-backward asymmetry, A_{FB} , for e^+e^- final states in $p\bar{p}$ collisions has been measured by CDF [131] and a value for \bar{s}_ℓ^2 has been extracted. By varying the invariant mass and the scattering angle (and assuming the electron couplings), the effective Z couplings to light quarks, $\bar{g}_{V,A}^{u,d}$, resulted, as well, but with large uncertainties and mutual correlations. A similar analysis has also been reported by the H1 Collaboration at HERA [132].

The electroweak radiative corrections have been absorbed into corrections $\rho_f - 1$ and $\kappa_f - 1$, which depend on the fermion f and on the renormalization scheme. In the on-shell scheme, the quadratic m_t dependence is given by $\rho_f \sim 1 + \rho_t$, $\kappa_f \sim 1 + \rho_t / \tan^2 \theta_W$, while in $\overline{\text{MS}}$, $\hat{\rho}_f \sim \hat{\kappa}_f \sim 1$, for $f \neq b$ ($\hat{\rho}_b \sim 1 - \frac{4}{3}\rho_t$, $\hat{\kappa}_b \sim 1 + \frac{2}{3}\rho_t$). In the $\overline{\text{MS}}$ scheme the normalization is changed according to $G_F M_Z^2 / 2\sqrt{2}\pi \rightarrow \hat{\alpha} / 4\hat{s}_Z^2 \hat{c}_Z^2$. (If one continues to normalize amplitudes by $G_F M_Z^2 / 2\sqrt{2}\pi$, as in the 1996 edition of this *Review*, then $\hat{\rho}_f$ contains an additional factor of $\hat{\rho}$.) In practice, additional bosonic and fermionic loops, vertex corrections, leading higher order contributions, *etc.*, must be included. For example, in the $\overline{\text{MS}}$ scheme one has $\hat{\rho}_\ell = 0.9981$, $\hat{\kappa}_\ell = 1.0013$, $\hat{\rho}_b = 0.9870$, and $\hat{\kappa}_b = 1.0067$. It is convenient to define an effective angle $\bar{s}_f^2 \equiv \sin^2 \bar{\theta}_{Wf} \equiv \hat{\kappa}_f \hat{s}_Z^2 = \kappa_f s_W^2$, in terms of which \bar{g}_V^f and \bar{g}_A^f are given by $\sqrt{\rho_f}$ times their tree-level formulae. Because \bar{g}_V^ℓ is very small, not only $A_{LR}^0 = A_e, A_{FB}^{(0,\ell)}$, and \mathcal{P}_τ , but also $A_{FB}^{(0,b)}, A_{FB}^{(0,c)}, A_{FB}^{(0,s)}$, and the hadronic asymmetries are mainly sensitive to \bar{s}_ℓ^2 . One finds that $\hat{\kappa}_f$ ($f \neq b$) is almost independent of (m_t, M_H) , so that one can write

$$\bar{s}_\ell^2 \sim \hat{s}_Z^2 + 0.00029. \quad (10.35)$$

Thus, the asymmetries determine values of \bar{s}_ℓ^2 and \hat{s}_Z^2 almost independent of m_t , while the κ 's for the other schemes are m_t dependent.

LEP 2 [45,130,133] ran at several energies above the Z -pole up to ~ 209 GeV. Measurements were made of a number of observables, including the cross-sections for $e^+e^- \rightarrow f\bar{f}$ for $f = q, \mu^-, \tau^-$; the differential cross-sections and A_{FB} for μ and τ ; R and A_{FB} for b and c ; W branching ratios; and $WW, WW\gamma, ZZ$, single W , and single Z cross-sections. They are in agreement with the SM predictions, with the exceptions of the total hadronic cross-section (1.7 σ high), R_b (2.1 σ low), and $A_{FB}(b)$ (1.6 σ low). Also, the SM Higgs boson was excluded below a mass of 114.4 GeV at the 95% CL [134].

The Z -boson properties are extracted assuming the SM expressions for the γ - Z interference terms. These have also been tested experimentally by performing more general fits [130,135] to the LEP 1 and LEP 2 data. Assuming family universality

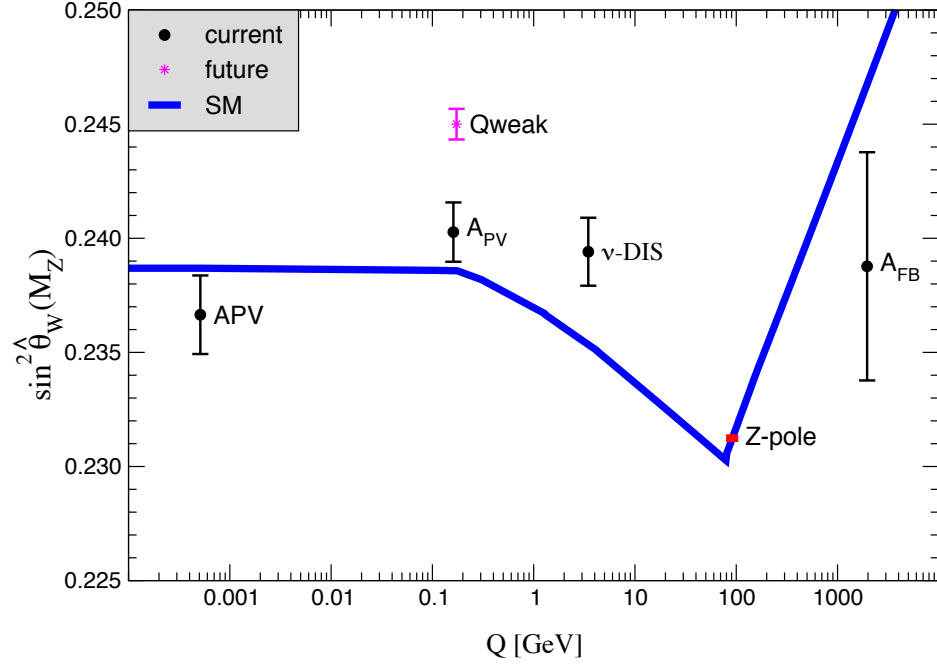


Figure 10.1: Scale dependence of the weak mixing angle defined in the $\overline{\text{MS}}$ scheme [137]. The minimum of the curve corresponds to $Q = M_W$, below which we switch to an effective theory with the W^\pm bosons integrated out, and where the β -function for the weak mixing angle changes sign. At the location of the W -boson mass and each fermion mass, there are also discontinuities arising from scheme dependent matching terms which are necessary to ensure that the various effective field theories within a given loop order describe the same physics. However, in the $\overline{\text{MS}}$ scheme these are very small numerically and barely visible in the figure provided one decouples quarks at $Q = \hat{m}_q(\hat{m}_q)$. The width of the curve reflects the SM uncertainty which is strongly dominated by the experimental error on \hat{s}_Z^2 . The theory uncertainty from strong interaction effects is at the level of $\pm 7 \times 10^{-5}$ [137]. See full-color version on color pages at end of book.

this approach introduces three additional parameters relative to the standard fit [45], describing the γ - Z interference contribution to the total hadronic and leptonic cross-sections, $j_{\text{had}}^{\text{tot}}$ and j_ℓ^{tot} , and to the leptonic forward-backward asymmetry, j_ℓ^{fb} . For example,

$$j_{\text{had}}^{\text{tot}} \sim g_V^\ell g_V^{\text{had}} = 0.277 \pm 0.065, \quad (10.36)$$

which is in good agreement with the SM expectation [45] of 0.21 ± 0.01 . Similarly, LEP data up to CM energies of 206 GeV are used to constrain the γ - Z interference terms for the heavy quarks. The results for j_b^{tot} , j_b^{fb} , j_c^{tot} , and j_c^{fb} were found in perfect agreement with the SM. These are valuable tests of the SM; but it should be cautioned that new physics is not expected to be described by this set of parameters, since (i) they do not account for extra interactions beyond the standard weak neutral-current, and (ii) the photonic amplitude remains fixed to its SM value.

18 10. Electroweak model and constraints on new physics

Strong constraints on anomalous triple and quartic gauge couplings have been obtained at LEP 2 and at the Tevatron, as are described in the Particle Listings.

The parity violating left-right asymmetry, A_{PV} , in fixed target polarized Møller scattering, $e^-e^- \rightarrow e^-e^-$, is defined as in Eq. (10.30) but with the opposite sign. It has been measured at low $Q^2 = 0.026 \text{ GeV}^2$ in the SLAC E158 experiment [136], with the result $A_{PV} = -1.31 \pm 0.14(\text{stat.}) \pm 0.10(\text{syst.}) \times 10^{-7}$. Expressed in terms of the weak mixing angle in the $\overline{\text{MS}}$ scheme, this yields $\hat{s}^2(Q^2) = 0.2403 \pm 0.0013$, and established the running of the weak mixing (see Fig. 10.1) at the level of 6.4 standard deviations. In a similar experiment and at about the same Q^2 , Qweak at Jefferson Lab [138] will be able to measure $\sin^2\theta_W$ in polarized ep scattering with a relative precision of 0.3%. These experiments will provide the most precise determinations of the weak mixing angle off the Z -peak and will be sensitive to various types of physics beyond the SM.

10.4. W and Z decays

The partial decay width for gauge bosons to decay into massless fermions $f_1\bar{f}_2$ (the numerical values include the small electroweak radiative corrections and final state mass effects) is

$$\Gamma(W^+ \rightarrow e^+\nu_e) = \frac{G_F M_W^3}{6\sqrt{2}\pi} \approx 226.29 \pm 0.16 \text{ MeV} \quad , \quad (10.44a)$$

$$\Gamma(W^+ \rightarrow u_i\bar{d}_j) = \frac{CG_F M_W^3}{6\sqrt{2}\pi} |V_{ij}|^2 \approx (706.24 \pm 0.49) |V_{ij}|^2 \text{ MeV} \quad , \quad (10.44b)$$

$$\Gamma(Z \rightarrow \psi_i\bar{\psi}_i) = \frac{CG_F M_Z^3}{6\sqrt{2}\pi} \left[g_V^{i2} + g_A^{i2} \right] \quad (10.44c)$$

$$\approx \begin{cases} 300.18 \pm 0.14 \text{ MeV} (u\bar{u}), & 167.21 \pm 0.05 \text{ MeV} (\nu\bar{\nu}), \\ 382.97 \pm 0.14 \text{ MeV} (d\bar{d}), & 83.99 \pm 0.03 \text{ MeV} (e^+e^-), \\ 375.95 \mp 0.10 \text{ MeV} (b\bar{b}). \end{cases}$$

For leptons $C = 1$, while for quarks $C = 3\left(1 + \alpha_s(M_V)/\pi + 1.409\alpha_s^2/\pi^2 - 12.77\alpha_s^3/\pi^3\right)$, where the 3 is due to color and the factor in parentheses represents the universal part of the QCD corrections [139] for massless quarks [140]. We also included the leading $\mathcal{O}(\alpha_s^4)$ contribution to hadronic Z decays [141]. The $Z \rightarrow f\bar{f}$ widths contain a number of additional corrections: universal (non-singlet) top quark mass contributions [142]; fermion mass effects and further QCD corrections proportional to $\hat{m}_q^2(M_Z^2)$ [143] which are different for vector and axial-vector partial widths; and singlet contributions starting from two-loop order which are large, strongly top quark mass dependent, family universal, and flavor non-universal [144]. All QCD effects are known and included up to three-loop order. The QED factor $1 + 3\alpha q_f^2/4\pi$, as well as two-loop order $\alpha\alpha_s$ and α^2 self-energy corrections [145] are also included. Working in the on-shell scheme, *i.e.*, expressing the widths in terms of $G_F M_{W,Z}^3$, incorporates the largest radiative corrections from the running QED coupling [49,146]. Electroweak corrections to the

Z -widths are then incorporated by replacing $g_{V,A}^{i2}$ by $\bar{g}_{V,A}^{i2}$. Hence, in the on-shell scheme the Z -widths are proportional to $\rho_i \sim 1 + \rho_t$. The $\overline{\text{MS}}$ normalization accounts also for the leading electroweak corrections [54]. There is additional (negative) quadratic m_t dependence in the $Z \rightarrow b\bar{b}$ vertex corrections [147] which causes $\Gamma(b\bar{b})$ to decrease with m_t . The dominant effect is to multiply $\Gamma(b\bar{b})$ by the vertex correction $1 + \delta\rho_{b\bar{b}}$, where $\delta\rho_{b\bar{b}} \sim 10^{-2}(-\frac{1}{2}\frac{m_t^2}{M_Z^2} + \frac{1}{5})$. In practice, the corrections are included in ρ_b and κ_b , as discussed before.

For 3 fermion families the total widths are predicted to be

$$\Gamma_Z \approx 2.4956 \pm 0.0007 \text{ GeV} \quad , \quad (10.45)$$

$$\Gamma_W \approx 2.0910 \pm 0.0015 \text{ GeV} \quad . \quad (10.46)$$

We have assumed $\alpha_s(M_Z) = 0.1200$. An uncertainty in α_s of ± 0.0017 introduces an additional uncertainty of 0.05% in the hadronic widths, corresponding to ± 0.8 MeV in Γ_Z . These predictions are to be compared with the experimental results $\Gamma_Z = 2.4952 \pm 0.0023$ GeV [45] and $\Gamma_W = 2.141 \pm 0.041$ GeV (see the Particle Listings for more details).

10.5. Precision flavor physics

In addition to cross-sections, asymmetries, parity violation, W and Z decays, there are a large number of experiments and observables testing the flavor structure of the SM. These are addressed elsewhere in this *Review*, and generally not included in this Section. However, we identify three precision observables with sensitivity to similar types of new physics as the other processes discussed here. The branching fraction of the flavor changing transition $b \rightarrow s\gamma$ is of comparatively low precision, but since it is a loop-level process (in the SM) its sensitivity to new physics (and SM parameters, such as heavy quark masses) is enhanced. The τ -lepton lifetime and leptonic branching ratios are primarily sensitive to α_s and not affected significantly by many types of new physics. However, having an independent and reliable low-energy measurement of α_s in a global analysis allows the comparison with the Z -lineshape determination of α_s which shifts easily in the presence of new physics contributions. By far the most precise observable discussed here is the anomalous magnetic moment of the muon (the electron magnetic moment is measured to even greater precision, but its new physics sensitivity is suppressed by terms proportional to m_e^2/M_Z^2). Its combined experimental and theoretical uncertainty is comparable to typical new physics contributions.

The CLEO [148], Belle [149], and BaBar [150] collaborations reported precise measurements of the process $b \rightarrow s\gamma$. We extrapolated these results to the full photon spectrum which is defined according to the recommendation in Ref. 151. The results for the branching fractions are then given by,

$$\begin{aligned} \text{CLEO} &: 3.34 \times 10^{-4} [1 \pm 0.134 \pm 0.076 \pm 0.038 \pm 0.048 \pm 0.006], \\ \text{Belle} &: 3.59 \times 10^{-4} [1 \pm 0.091_{-0.084}^{+0.081} \pm 0.025 \pm 0.020 \pm 0.006], \\ \text{BaBar} &: 4.01 \times 10^{-4} [1 \pm 0.080 \pm 0.091 \pm 0.079 \pm 0.026 \pm 0.006], \\ \text{BaBar} &: 3.57 \times 10^{-4} [1 \pm 0.055_{-0.122}^{+0.168} \pm 0.000 \pm 0.026 \pm 0.000], \end{aligned}$$

20 10. Electroweak model and constraints on new physics

where the first two errors are the statistical and systematic uncertainties (taken uncorrelated). In the case of CLEO, a 3.8% component from the model error of the signal efficiency is moved from the systematic error to the model (third) error. The fourth error accounts for the extrapolation from the finite photon energy cutoff [151–153] (2.0 GeV, 1.815 GeV, and 1.9 GeV, respectively, for CLEO, Belle, and BaBar) to the full theoretical branching ratio. For this we use the results of Ref. 151 for $m_b = 4.70$ GeV which is in good agreement with the more recent Ref. 153. The uncertainty reflects the difference due to choosing $m_b = 4.80$ GeV, instead. The last error is from the correction (0.962 ± 0.006) for the $b \rightarrow d\gamma$ component which is common to all inclusive measurements, but absent for the exclusive BaBar measurement in the last line. The last three errors are taken as 100% correlated, resulting in the correlation matrix in Table 10.4. It is advantageous [154] to normalize the result with respect to the semi-leptonic branching fraction, $\mathcal{B}(b \rightarrow X e \nu) = 0.1087 \pm 0.0017$, yielding,

$$R = \frac{\mathcal{B}(b \rightarrow s\gamma)}{\mathcal{B}(b \rightarrow X e \nu)} = (3.34 \pm 0.28 \pm 0.37) \times 10^{-3}. \quad (10.47)$$

In the fits we use the variable $\ln R = -5.70 \pm 0.14$ to assure an approximately Gaussian error [155]. The second uncertainty in Eq. (10.47) is an 11% theory uncertainty (excluding parametric errors such as from α_s) in the SM prediction which is based on the next-to-leading order calculations of Refs. 154,156.

Table 10.4: Correlation matrix for measurements of the $b \rightarrow s\gamma$ transition.

CLEO	1.000	0.092	0.176	0.048
Belle	0.092	1.000	0.136	0.026
BaBar (inclusive)	0.176	0.136	1.000	0.029
BaBar (exclusive)	0.048	0.026	0.029	1.000

The extraction of α_s from the τ lifetime and leptonic branching ratios is standing out from other determinations, because of a variety of independent reasons: (i) the τ -scale is low, so that upon extrapolation to the Z -scale (where it can be compared to the theoretically clean Z -lineshape determinations) the α_s error shrinks by about an order of magnitude; (ii) yet, this scale is high enough that perturbation theory and the operator product expansion (OPE) can be applied; (iii) these observables are fully inclusive and thus free of fragmentation and hadronization effects that would have to be modeled or measured; (iv) OPE breaking effects are most problematic near the branch cut but there they are suppressed by a double zero at $s = m_\tau^2$; (v) there are enough data [19] to constrain non-perturbative effects both within and breaking the OPE; (vi) a complete three-loop order QCD calculation is available; (vii) large effects associated with the QCD β -function can be resummed [157] (in what has become known as contour

improvement) and these have been computed to even four-loop precision [158]. The largest uncertainty is from the missing perturbative four and higher loop coefficients (appearing in the Adler- D function). The corresponding effects are highly non-linear so that this uncertainty is itself α_s dependent, updated in each call of the fits, and leading to an asymmetric error. The second largest uncertainty is from the missing perturbative five and higher loop coefficients of the QCD β -function; this induces an uncertainty in the contour improvement which is fully correlated with the renormalization group extrapolation from the τ to the Z -scale. The third largest error is from the experimental uncertainty in the lifetime, $\tau_\tau = 290.89 \pm 0.58$ fs, which is from the two leptonic branching ratios and the direct τ_τ . Because of the poor convergence of perturbation theory for strange quark final states, we used for these the experimentally measured branching ratio. Included are also various smaller uncertainties from other sources. In total we obtain a 2% determination of $\alpha_s(M_Z) = 0.1225^{+0.0025}_{-0.0022}$ which updates the result of Ref. 5. For more details, see Ref. 19 where even 1–1.5% uncertainties are advocated (mainly by means of additional assumptions regarding the perturbative four-loop error).

The world average of the muon anomalous magnetic moment*,

$$a_\mu^{\text{exp}} = \frac{g_\mu - 2}{2} = (1165920.80 \pm 0.63) \times 10^{-9}, \quad (10.48)$$

is dominated by the 1999, 2000, and 2001 data runs of the E821 collaboration at BNL [159]. The QED contribution has been calculated to four loops [160] (fully analytically to three loops [161,162]), and the leading logarithms are included to five loops [163,164]. The estimated SM electroweak contribution [165–167], $a_\mu^{\text{EW}} = (1.52 \pm 0.03) \times 10^{-9}$, which includes leading two-loop [166] and three-loop [167] corrections, is at the level of the current uncertainty. The limiting factor in the interpretation of the result is the uncertainty from the two-loop hadronic contribution [20], $a_\mu^{\text{had}} = (69.54 \pm 0.64) \times 10^{-9}$, which has been obtained using $e^+e^- \rightarrow$ hadrons cross-section data (including the KLOE data from radiative returns from the Φ resonance [42] and the very recent SND data [39]). The latter are dominated by the (reanalyzed) CMD 2 data [17]. This value suggests a 2.3 σ discrepancy between Eq. (10.48) and the SM prediction. In an alternative analysis, the authors of Ref. 18 used τ decay data and isospin symmetry (CVC) to obtain $a_\mu^{\text{had}} = (71.10 \pm 0.58) \times 10^{-9}$. This result implies no conflict (0.7 σ) with Eq. (10.48). Thus, there is also a discrepancy between the 2π and 4π spectral functions obtained from the two methods. For example, if one uses the e^+e^- data and CVC to predict the branching ratio for $\tau^- \rightarrow \nu_\tau \pi^- \pi^0$ decays one obtains $24.52 \pm 0.31\%$ [20] (this

* In what follows, we summarize the most important aspects of $g_\mu - 2$, and give some details about the evaluation in our fits. For more details see the dedicated contribution by A. Höcker and W. Marciano in this *Review*. There are some small numerical differences (at the level of 0.1 standard deviation), which are well understood and mostly arise because internal consistency of the fits requires the calculation of all observables from analytical expressions and common inputs and fit parameters, so that an independent evaluation is necessary for this Section. Note, that in the spirit of a global analysis based on all available information we have chosen here to average in the τ -decay data, as well.

22 10. Electroweak model and constraints on new physics

does not include the SND data) while the average of the measured branching ratios by DELPHI [168], ALEPH, CLEO, L3, and OPAL [18] yields $25.43 \pm 0.09\%$, which is 2.8σ higher. It is important to understand the origin of this difference, but four observations point to the conclusion that at least some of it is experimental: (i) Including the SND data in the e^+e^- data set (which are consistent with the implications of the τ decay data), this discrepancy decreases to about 2.4σ (in particular, the KLOE and SND results differ both qualitatively and quantitatively), and would decrease further if the older data are discarded. (ii) The $\tau^- \rightarrow \nu_\tau 2\pi^- \pi^+ \pi^0$ spectral function also disagrees with the corresponding e^+e^- data at the 4σ level, which translates to a 23% effect [20] and seems too large to arise from isospin violation. (iii) Isospin violating corrections have been studied in detail in Ref. 169 and found to be largely under control. The largest effect is due to higher-order electroweak corrections [43] but introduces a negligible uncertainty [170]. (iv) Ref. 171 shows on the basis of a QCD sum rule that the spectral functions derived from τ decay data are consistent with values of $\alpha_s(M_Z) \gtrsim 0.120$, in agreement with what we find from the global fit in Sec. 10.6, while the spectral functions from e^+e^- annihilation are consistent only for somewhat lower (disfavored) values. Nevertheless, a_μ^{had} has been evaluated in Refs. 36,172 excluding the τ decay data with results which are generally in good agreement with each other and other e^+e^- based analyzes. It is argued [172] that CVC breaking effects (*e.g.*, through a relatively large mass difference between the ρ^\pm and ρ^0 vector mesons) may be larger than expected. (This may also be relevant in the context of the NuTeV discrepancy discussed above [172].) Experimentally [19], this mass difference is indeed larger than expected, but then one would also expect a significant width difference which is contrary to observation [19]. Fortunately, due to the suppression at large s (from where the conflicts originate) these problems are less pronounced as far as a_μ^{had} is concerned. In the following we view all differences in spectral functions as fluctuations and average the results. An additional uncertainty is induced by the hadronic three-loop light-by-light scattering contribution. We use the most recent value [173], $a_\mu^{\text{LBS}} = (+1.36 \pm 0.25) \times 10^{-9}$, which is higher than previous evaluations [174,175]. The sign of this effect is opposite [174] to the one quoted in the 2002 edition of this *Review*, and has subsequently been confirmed by two other groups [175]. Other hadronic effects at three-loop order contribute [176], $a_\mu^{\text{had}} \left[\left(\frac{\alpha}{\pi} \right)^3 \right] = (-1.00 \pm 0.06) \times 10^{-9}$. Correlations with the two-loop hadronic contribution and with $\Delta\alpha(M_Z)$ (see Sec. 10.2) were considered in Ref. 162, which also contains analytic results for the perturbative QCD contribution. The SM prediction is

$$a_\mu^{\text{theory}} = (1165919.52 \pm 0.52) \times 10^{-9} , \quad (10.49)$$

where the error is from the hadronic uncertainties excluding parametric ones such as from α_s and the heavy quark masses. We estimate its correlation with $\Delta\alpha(M_Z)$ as 24%. The small overall discrepancy between the experimental and theoretical values could be due to fluctuations or underestimates of the theoretical uncertainties. On the other hand, $g_\mu - 2$ is also affected by many types of new physics, such as supersymmetric models with large $\tan\beta$ and moderately light superparticle masses [177]. Thus, the deviation could also

arise from physics beyond the SM.

Table 10.5: Principal Z -pole and other observables, compared with the SM best fit predictions (see text). The LEP averages of the ALEPH, DELPHI, L3, and OPAL results include common systematic errors and correlations [45]. The heavy flavor results of LEP and SLD are based on common inputs and correlated, as well [45]. The first $\bar{s}_\ell^2(A_{FB}^{(0,q)})$ is the effective angle extracted from the hadronic charge asymmetry, which has some (neglected) correlation with $A_{FB}^{(0,b)}$; the second $\bar{s}_\ell^2(A_{FB}^{(0,q)})$ is from the lepton asymmetry from CDF [131]. The values of $\Gamma(\ell^+\ell^-)$, $\Gamma(\text{had})$, and $\Gamma(\text{inv})$ are not independent of Γ_Z , the R_ℓ , and σ_{had} . The first M_W value is from UA2, CDF, and DØ [178], and based on the two-parameter analysis of Ref. 179; the second one is from LEP 2 [180]. The first M_W and M_Z are correlated, but the effect is negligible due to the tiny M_Z error. The three values of A_e are (i) from A_{LR} for hadronic final states [125]; (ii) from A_{LR} for leptonic final states and from polarized Bhabba scattering [127]; and (iii) from the angular distribution of the τ polarization. The two A_τ values are from SLD and the total τ polarization, respectively. g_L^2 and g_R^2 are from NuTeV [82] and have a very small (-1.7%) residual anti-correlation. The older deep-inelastic scattering (DIS) results from CDHS [75], CHARM [76], and CCFR [77] are included, as well, but not shown in the Table. The world averages for $g_{V,A}^{\nu e}$ are dominated by the CHARM II [99] results, $g_V^{\nu e} = -0.035 \pm 0.017$ and $g_A^{\nu e} = -0.503 \pm 0.017$. A_{PV} is the parity violating asymmetry in Møller scattering. The errors in Q_W , DIS, $b \rightarrow s\gamma$, and $g_\mu - 2$ are the total (experimental plus theoretical) uncertainties. The τ_τ value is the τ lifetime world average computed by combining the direct measurements with values derived from the leptonic branching ratios [5]; the theory uncertainty is included in the SM prediction. In all other SM predictions, the uncertainty is from M_Z , M_H , m_t , m_b , m_c , $\hat{\alpha}(M_Z)$, and α_s , and their correlations have been accounted for. The SM errors in Γ_Z , $\Gamma(\text{had})$, R_ℓ , and σ_{had} are largely dominated by the uncertainty in α_s .

Quantity	Value	Standard Model	Pull
m_t [GeV]	$172.7 \pm 2.9 \pm 0.6$	172.7 ± 2.8	0.0
M_W [GeV]	80.450 ± 0.058	80.376 ± 0.017	1.3
	80.392 ± 0.039		0.4
M_Z [GeV]	91.1876 ± 0.0021	91.1874 ± 0.0021	0.1
Γ_Z [GeV]	2.4952 ± 0.0023	2.4968 ± 0.0011	-0.7
$\Gamma(\text{had})$ [GeV]	1.7444 ± 0.0020	1.7434 ± 0.0010	—
$\Gamma(\text{inv})$ [MeV]	499.0 ± 1.5	501.65 ± 0.11	—
$\Gamma(\ell^+\ell^-)$ [MeV]	83.984 ± 0.086	83.996 ± 0.021	—
σ_{had} [nb]	41.541 ± 0.037	41.467 ± 0.009	2.0
R_e	20.804 ± 0.050	20.756 ± 0.011	1.0
R_μ	20.785 ± 0.033	20.756 ± 0.011	0.9
R_τ	20.764 ± 0.045	20.801 ± 0.011	-0.8
R_b	0.21629 ± 0.00066	0.21578 ± 0.00010	0.8
R_c	0.1721 ± 0.0030	0.17230 ± 0.00004	-0.1
$A_{FB}^{(0,e)}$	0.0145 ± 0.0025	0.01622 ± 0.00025	-0.7
$A_{FB}^{(0,\mu)}$	0.0169 ± 0.0013		0.5
$A_{FB}^{(0,\tau)}$	0.0188 ± 0.0017		1.5
$A_{FB}^{(0,b)}$	0.0992 ± 0.0016	0.1031 ± 0.0008	-2.4
$A_{FB}^{(0,c)}$	0.0707 ± 0.0035	0.0737 ± 0.0006	-0.8
$A_{FB}^{(0,s)}$	0.0976 ± 0.0114	0.1032 ± 0.0008	-0.5
$\bar{s}_\ell^2(A_{FB}^{(0,q)})$	0.2324 ± 0.0012	0.23152 ± 0.00014	0.7
	0.2238 ± 0.0050		-1.5
A_e	0.15138 ± 0.00216	0.1471 ± 0.0011	2.0
	0.1544 ± 0.0060		1.2
	0.1498 ± 0.0049		0.6
A_μ	0.142 ± 0.015		-0.3
A_τ	0.136 ± 0.015		-0.7
	0.1439 ± 0.0043		-0.7
A_b	0.923 ± 0.020	0.9347 ± 0.0001	-0.6
A_c	0.670 ± 0.027	0.6678 ± 0.0005	0.1
A_s	0.895 ± 0.091	0.9356 ± 0.0001	-0.4
g_L^2	0.30005 ± 0.00137	0.30378 ± 0.00021	-2.7
g_R^2	0.03076 ± 0.00110	0.03006 ± 0.00003	0.6
$g_V^{\nu e}$	-0.040 ± 0.015	-0.0396 ± 0.0003	0.0
$g_A^{\nu e}$	-0.507 ± 0.014	-0.5064 ± 0.0001	0.0
A_{PV}	-1.31 ± 0.17	-1.53 ± 0.02	1.3
$Q_W(\text{Cs})$	-72.62 ± 0.46	-73.17 ± 0.03	1.2
$Q_W(\text{Tl})$	-116.6 ± 3.7	-116.78 ± 0.05	0.1
$\frac{\Gamma(b \rightarrow s\gamma)}{\Gamma(b \rightarrow X e \nu)}$	$3.35_{-0.44}^{+0.50} \times 10^{-3}$	$(3.22 \pm 0.09) \times 10^{-3}$	0.3
$\frac{1}{2}(g_\mu - 2 - \frac{\alpha}{\pi})$	4511.07 ± 0.82	4509.82 ± 0.10	1.5
τ_τ [fs]	290.89 ± 0.58	291.87 ± 1.76	-0.4

10.6. Experimental results

The values of the principal Z -pole observables are listed in Table 10.5, along with the SM predictions for $M_Z = 91.1874 \pm 0.0021$ GeV, $M_H = 89_{-28}^{+38}$ GeV, $m_t = 172.7 \pm 2.8$ GeV, $\alpha_s(M_Z) = 0.1216 \pm 0.0017$, and $\hat{\alpha}(M_Z)^{-1} = 127.904 \pm 0.019$ ($\Delta\alpha_{\text{had}}^{(5)} \approx 0.02802 \pm 0.00015$). The predictions result from a global least-square (χ^2) fit to all data using the minimization package MINUIT [181] and the electroweak library GAPP [73]. In most cases, we treat all input errors (the uncertainties of the values) as Gaussian. The reason is not that we assume that theoretical and systematic errors are intrinsically bell-shaped (which they are not) but because in most cases the input errors are combinations of many different (including statistical) error sources, which should yield approximately Gaussian *combined* errors by the large number theorem. Thus, it suffices if either the statistical components dominate or there are many components of similar size. An exception is the theory dominated error on the τ lifetime, which we recalculate in each χ^2 -function call since it depends itself on α_s yielding an asymmetric (and thus non-Gaussian) error bar. Sizes and shapes of the output errors (the uncertainties of the predictions and the SM fit parameters) are fully determined by the fit, and 1σ errors are defined to correspond to $\Delta\chi^2 = \chi^2 - \chi_{\text{min}}^2 = 1$, and do not necessarily correspond to the 68.3% probability range or the 39.3% probability contour (for 2 parameters).

Table 10.6: Principal SM fit result including mutual correlations.

M_Z [GeV]	91.1874 ± 0.0021	1.00	-0.02	0.00	0.00	-0.01	0.00	0.08
m_t [GeV]	172.7 ± 2.8	-0.02	1.00	0.00	0.00	-0.03	-0.02	0.61
$\hat{m}_b(\hat{m}_b)$ [GeV]	4.207 ± 0.031	0.00	0.00	1.00	0.29	-0.03	0.01	0.05
$\hat{m}_c(\hat{m}_c)$ [GeV]	$1.290_{-0.045}^{+0.040}$	0.00	0.00	0.29	1.00	0.09	0.03	0.14
$\alpha_s(M_Z)$	0.1216 ± 0.0017	-0.01	-0.03	-0.03	0.09	1.00	-0.01	-0.02
$\Delta\alpha_{\text{had}}^{(3)}$ (1.8 GeV)	0.00581 ± 0.00010	0.00	-0.02	0.01	0.03	-0.01	1.00	-0.18
M_H [GeV]	89_{-28}^{+38} GeV	0.08	0.61	0.05	0.14	-0.02	-0.18	1.00

The values and predictions of m_t [6–8]; M_W [178–180]; deep inelastic [82], ν_μ - e [97–99], and polarized Møller scattering [136]; the Q_W for cesium [105,106] and thallium [107]; the $b \rightarrow s\gamma$ observable [148–150]; the muon anomalous magnetic moment [159]; and the τ lifetime are also listed in Table 10.5. The values of M_W and m_t differ from those in the Particle Listings because they include recent preliminary results. The agreement is excellent. Despite the discrepancies discussed in the following, the goodness of the fit to all data is very good with a $\chi^2/\text{d.o.f.} = 47.5/42$. The probability of a larger χ^2 is 26%. Only g_L^2 from NuTeV and $A_{FB}^{(0,b)}$ from LEP are currently showing large (2.7σ and 2.4σ) deviations. In addition, the hadronic peak cross-section, σ_{had} (LEP), and

26 10. Electroweak model and constraints on new physics

the A_{LR}^0 (SLD) from hadronic final states differ by 2.0σ . The final result for $g_\mu - 2$ from BNL has moved up, and so has the SM prediction due to the higher value of the light-by-light contribution [173], so that the small net deviation (1.5σ , see Sec. 10.5) is basically unchanged compared to the 2004 edition of this *Review*. Observables like $R_b = \Gamma(b\bar{b})/\Gamma(\text{had})$, $R_c = \Gamma(c\bar{c})/\Gamma(\text{had})$, and the combined value for M_W which showed significant deviations in the past, are now in reasonable agreement. In particular, R_b , whose measured value deviated by as much as 3.7σ from the SM prediction, is now in agreement.

A_b can be extracted from $A_{FB}^{(0,b)}$ when $A_e = 0.1501 \pm 0.0016$ is taken from a fit to leptonic asymmetries (using lepton universality). The result, $A_b = 0.881 \pm 0.017$, is 3.1σ below the SM prediction[†], and also 1.6σ below $A_b = 0.923 \pm 0.020$ obtained from $A_{LR}^{FB}(b)$ at SLD. Thus, it appears that at least some of the problem in $A_{FB}^{(0,b)}$ is experimental. Note, however, that the uncertainty in $A_{FB}^{(0,b)}$ is strongly statistics dominated. The combined value, $A_b = 0.899 \pm 0.013$ deviates by 2.8σ . It would be extremely difficult to account for this 3.9% deviation by new physics radiative corrections since about a 20% correction to $\hat{\kappa}_b$ would be necessary to account for the central value of A_b . If this deviation is due to new physics, it is most likely of tree-level type affecting preferentially the third generation. Examples include the decay of a scalar neutrino resonance [182], mixing of the b quark with heavy exotics [183], and a heavy Z' with family-nonuniversal couplings [184]. It is difficult, however, to simultaneously account for R_b , which has been measured on the Z -peak and off-peak [185] at LEP 1. An average of R_b measurements at LEP 2 at energies between 133 and 207 GeV is 2.1σ below the SM prediction, while $A_{FB}^{(b)}$ (LEP 2) is 1.6σ low [133].

The left-right asymmetry, $A_{LR}^0 = 0.15138 \pm 0.00216$ [125], based on all hadronic data from 1992–1998 differs 2.0σ from the SM expectation of 0.1471 ± 0.0011 . The combined value of $A_\ell = 0.1513 \pm 0.0021$ from SLD (using lepton-family universality and including correlations) is also 2.0σ above the SM prediction; but there is now experimental agreement between this SLD value and the LEP value, $A_\ell = 0.1481 \pm 0.0027$, obtained from a fit to $A_{FB}^{(0,\ell)}$, $A_e(\mathcal{P}_\tau)$, and $A_\tau(\mathcal{P}_\tau)$, again assuming universality.

The observables in Table 10.5, as well as some other less precise observables, are used in the global fits described below. The correlations on the LEP lineshape and τ polarization, the LEP/SLD heavy flavor observables, the SLD lepton asymmetries, and the deep inelastic and ν - e scattering observables, are included. The theoretical correlations between $\Delta\alpha_{\text{had}}^{(5)}$ and $g_\mu - 2$, and between the charm and bottom quark masses, are also accounted for.

The data allow a simultaneous determination of M_H , m_t , $\sin^2 \theta_W$, and the strong coupling $\alpha_s(M_Z)$. (\hat{m}_c , \hat{m}_b , and $\Delta\alpha_{\text{had}}^{(5)}$ are also allowed to float in the fits, subject to the theoretical constraints [5,16] described in Sec. 10.1–Sec. 10.2. These are correlated with

[†] Alternatively, one can use $A_\ell = 0.1481 \pm 0.0027$, which is from LEP alone and in excellent agreement with the SM, and obtain $A_b = 0.893 \pm 0.022$ which is 1.9σ low. This illustrates that some of the discrepancy is related to the one in A_{LR} .

α_s .) α_s is determined mainly from R_ℓ , Γ_Z , σ_{had} , and τ_τ and is only weakly correlated with the other variables (except for a 9% correlation with \widehat{m}_c). The global fit to all data, including the CDF/DØ average, $m_t = 172.7 \pm 3.0$ GeV, yields

$$\begin{aligned} M_H &= 89_{-28}^{+38} \text{ GeV} , \\ m_t &= 172.7 \pm 2.8 \text{ GeV} , \\ \widehat{s}_Z^2 &= 0.23122 \pm 0.00015 , \\ \alpha_s(M_Z) &= 0.1216 \pm 0.0017 . \end{aligned} \tag{10.50}$$

The complete fit result including the correlation matrix is given in Table 10.6.

In the on-shell scheme one has $s_W^2 = 0.22306 \pm 0.00033$, the larger error due to the stronger sensitivity to m_t , while the corresponding effective angle is related by Eq. (10.35), *i.e.*, $\overline{s}_\ell^2 = 0.23152 \pm 0.00014$. The m_t pole mass corresponds to $\widehat{m}_t(\widehat{m}_t) = 162.7 \pm 2.7$ GeV. In all fits, the errors include full statistical, systematic, and theoretical uncertainties. The \widehat{s}_Z^2 (\overline{s}_ℓ^2) error reflects the error on $\overline{s}_\ell^2 = 0.23152 \pm 0.00016$ from a fit to the Z -pole asymmetries (including the CDF lepton asymmetry [131]).

As described at the beginning of Sec. 10.2 and the last paragraph of Sec. 10.5, there is some spread in the experimental e^+e^- spectral functions and also some stress when these are compared with τ -decay spectral functions. These are below or above the 2σ level (depending on what is actually compared) but not larger than the deviations of some other quantities entering our analyzes. The number and size of these deviations are well consistent with what one would expect to happen as a result of random fluctuations. It is nevertheless instructive to study the effect of doubling the uncertainty in $\Delta\alpha_{\text{had}}^{(3)}(1.8 \text{ GeV}) = 0.00577 \pm 0.00010$ (see the beginning of Sec. 10.2) on the extracted Higgs mass. The result, $M_H = 87_{-29}^{+39}$ GeV, demonstrates that the uncertainty in $\Delta\alpha_{\text{had}}$ is currently of only secondary importance. Note also, that the uncertainty of ± 0.0001 in $\Delta\alpha_{\text{had}}^{(3)}(1.8 \text{ GeV})$ corresponds to a shift of ∓ 6 GeV in M_H or less than one fifth of its total uncertainty.

The weak mixing angle can be determined from Z -pole observables, M_W , and from a variety of neutral-current processes spanning a very wide Q^2 range. The results (for the older low-energy neutral-current data see [46,47]) shown in Table 10.7 are in reasonable agreement with each other, indicating the quantitative success of the SM. The largest discrepancy is the value $\widehat{s}_Z^2 = 0.2355 \pm 0.0016$ from DIS which is 2.7σ above the value 0.23122 ± 0.00015 from the global fit to all data. Similarly, $\widehat{s}_Z^2 = 0.23193 \pm 0.00028$ from the forward-backward asymmetries into bottom and charm quarks, and $\widehat{s}_Z^2 = 0.23067 \pm 0.00029$ from the SLD asymmetries (both when combined with M_Z) are 2.5σ high and 1.9σ low, respectively.

The extracted Z -pole value of $\alpha_s(M_Z)$ is based on a formula with negligible theoretical uncertainty (± 0.0005 in $\alpha_s(M_Z)$) if one assumes the exact validity of the SM. One should keep in mind, however, that this value, $\alpha_s = 0.1198 \pm 0.0028$, is very sensitive to such types of new physics as non-universal vertex corrections. In contrast, the value derived from τ decays, $\alpha_s(M_Z) = 0.1225_{-0.0022}^{+0.0025}$, is theory dominated but less sensitive to new

Table 10.7: Values of \widehat{s}_Z^2 , s_W^2 , α_s , and M_H [in GeV] for various (combinations of) observables. Unless indicated otherwise, the top quark mass, $m_t = 172.7 \pm 3.0$ GeV, is used as an additional constraint in the fits. The (†) symbol indicates a fixed parameter.

Data	\widehat{s}_Z^2	s_W^2	$\alpha_s(M_Z)$	M_H
All data	0.23122(15)	0.22306(33)	0.1216(17)	89_{-28}^{+38}
All indirect (no m_t)	0.23122(16)	0.22307(41)	0.1216(17)	87_{-43}^{+107}
Z pole (no m_t)	0.23121(17)	0.22310(59)	0.1198(28)	89_{-44}^{+112}
LEP 1 (no m_t)	0.23152(21)	0.22375(67)	0.1213(30)	168_{-91}^{+232}
SLD + M_Z	0.23067(29)	0.22203(56)	0.1216 (†)	28_{-16}^{+26}
$A_{FB}^{(b,c)} + M_Z$	0.23193(28)	0.22480(76)	0.1216 (†)	349_{-148}^{+250}
$M_W + M_Z$	0.23089(38)	0.22241(74)	0.1216 (†)	47_{-31}^{+52}
M_Z	0.23134(11)	0.22334(36)	0.1216 (†)	117 (†)
polarized Møller	0.2330(14)	0.2251(14)	0.1216 (†)	117 (†)
DIS (isoscalar)	0.2355(16)	0.2275(16)	0.1216 (†)	117 (†)
Q_W (APV)	0.2290(19)	0.2210(19)	0.1216 (†)	117 (†)
elastic $\nu_\mu(\overline{\nu}_\mu)e$	0.2310(77)	0.2230(77)	0.1216 (†)	117 (†)
SLAC eD	0.222(18)	0.213(19)	0.1216 (†)	117 (†)
elastic $\nu_\mu(\overline{\nu}_\mu)p$	0.211(33)	0.203(33)	0.1216 (†)	117 (†)

physics. The two values are in remarkable agreement with each other. They are also in perfect agreement with other recent values, such as from jet-event shapes at LEP [186] (0.1202 ± 0.0050) and HERA [187] (0.1186 ± 0.0051), but the τ decay result is somewhat higher than the value, 0.1170 ± 0.0012 , from the most recent unquenched lattice calculation of Ref. 188. For more details and other determinations, see our Section 9 on “Quantum Chromodynamics” in this *Review*.

The data indicate a preference for a small Higgs mass. There is a strong correlation between the quadratic m_t and logarithmic M_H terms in $\widehat{\rho}$ in all of the indirect data except for the $Z \rightarrow b\bar{b}$ vertex. Therefore, observables (other than R_b) which favor m_t values higher than the Tevatron range favor lower values of M_H . This effect is enhanced by R_b , which has little direct M_H dependence but favors the lower end of the Tevatron m_t range. M_W has additional M_H dependence through $\Delta\widehat{r}_W$ which is not coupled to m_t^2 effects. The strongest individual pulls toward smaller M_H are from M_W and A_{LR}^0 , while $A_{FB}^{(0,b)}$ and the NuTeV results favor high values. The difference in χ^2 for the global fit is

$\Delta\chi^2 = \chi^2(M_H = 1000 \text{ GeV}) - \chi_{\min}^2 = 60$. Hence, the data favor a small value of M_H , as in supersymmetric extensions of the SM. The central value of the global fit result, $M_H = 89_{-28}^{+38} \text{ GeV}$, is below the direct lower bound, $M_H \geq 114.4 \text{ GeV}$ (95% CL) [134].

The 90% central confidence range from all precision data is

$$46 \text{ GeV} \leq M_H \leq 154 \text{ GeV} .$$

Including the results of the direct searches as an extra contribution to the likelihood function drives the 95% upper limit to $M_H \leq 189 \text{ GeV}$. As two further refinements, we account for (i) theoretical uncertainties from uncalculated higher order contributions by allowing the T parameter (see next subsection) subject to the constraint $T = 0 \pm 0.02$, (ii) the M_H dependence of the correlation matrix which gives slightly more weight to lower Higgs masses [189]. The resulting limits at 95 (90, 99)% CL are

$$M_H \leq 194 (176, 235) \text{ GeV} ,$$

respectively. The extraction of M_H from the precision data depends strongly on the value used for $\alpha(M_Z)$. Upper limits, however, are more robust due to two compensating effects: the older results indicated more QED running and were less precise, yielding M_H distributions which were broader with centers shifted to smaller values. The hadronic contribution to $\alpha(M_Z)$ is correlated with $g_\mu - 2$ (see Sec. 10.5). The measurement of the latter is higher than the SM prediction, and its inclusion in the fit favors a larger $\alpha(M_Z)$ and a lower M_H (by 3 GeV).

One can also carry out a fit to the indirect data alone, *i.e.*, without including the constraint, $m_t = 172.7 \pm 3.0 \text{ GeV}$, obtained by CDF and DØ. (The indirect prediction is for the $\overline{\text{MS}}$ mass, $\hat{m}_t(\hat{m}_t) = 162.4_{-7.2}^{+9.6} \text{ GeV}$, which is in the end converted to the pole mass). One obtains $m_t = 172.3_{-7.6}^{+10.2} \text{ GeV}$, with almost no change in the $\sin^2 \theta_W$ and α_s values, in perfect agreement with the direct CDF/DØ average. The relations between M_H and m_t for various observables are shown in Fig. 10.2.

Using $\alpha(M_Z)$ and \hat{s}_Z^2 as inputs, one can predict $\alpha_s(M_Z)$ assuming grand unification. One predicts [190] $\alpha_s(M_Z) = 0.130 \pm 0.001 \pm 0.01$ for the simplest theories based on the minimal supersymmetric extension of the SM, where the first (second) uncertainty is from the inputs (thresholds). This is slightly larger, but consistent with the experimental $\alpha_s(M_Z) = 0.1216 \pm 0.0017$ from the Z -lineshape and the τ lifetime, as well as with other determinations. Non-supersymmetric unified theories predict the low value $\alpha_s(M_Z) = 0.073 \pm 0.001 \pm 0.001$. See also the note on “Low-Energy Supersymmetry” in the Particle Listings.

One can also determine the radiative correction parameters Δr : from the global fit one obtains $\Delta r = 0.0355 \pm 0.0010$ and $\Delta \hat{r}_W = 0.06959 \pm 0.00029$. M_W measurements [178–180] (when combined with M_Z) are equivalent to measurements of $\Delta r = 0.0335 \pm 0.0020$, which is 1.2σ below the result from all indirect data, $\Delta r = 0.0362 \pm 0.0012$. Fig. 10.3 shows the 1σ contours in the $M_W - m_t$ plane from the direct and indirect determinations, as well as the combined 90% CL region. The indirect determination uses M_Z from LEP 1 as input, which is defined assuming an s dependent decay width. M_W then corresponds to the s

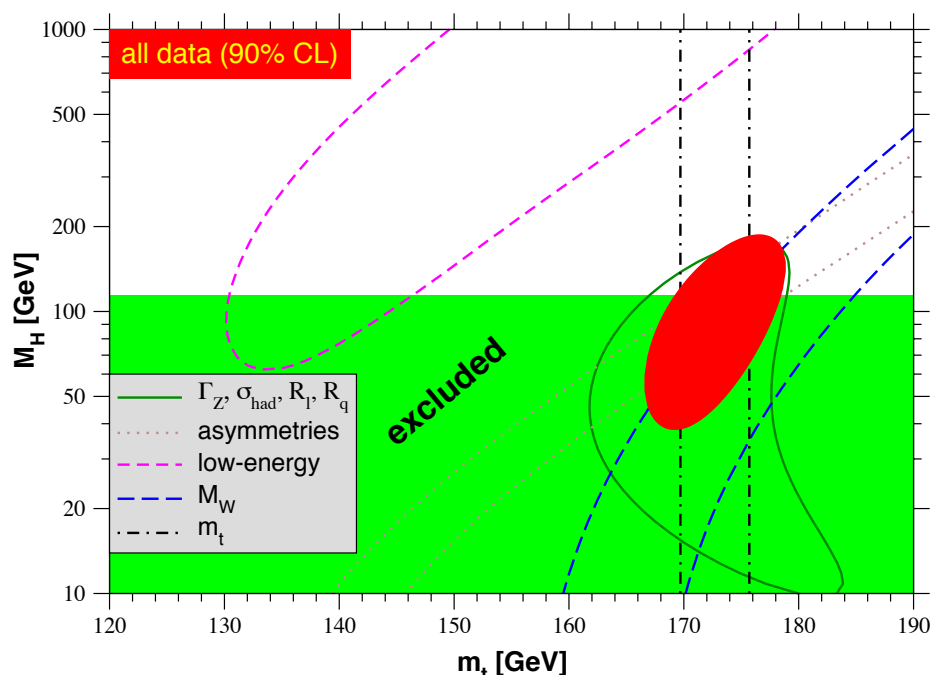


Figure 10.2: One-standard-deviation (39.35%) uncertainties in M_H as a function of m_t for various inputs, and the 90% CL region ($\Delta\chi^2 = 4.605$) allowed by all data. $\alpha_s(M_Z) = 0.120$ is assumed except for the fits including the Z -lineshape data. The 95% direct lower limit from LEP 2 is also shown. See full-color version on color pages at end of book.

dependent width definition, as well, and can be directly compared with the results from the Tevatron and LEP 2 which have been obtained using the same definition. The difference to a constant width definition is formally only of $\mathcal{O}(\alpha^2)$, but is strongly enhanced since the decay channels add up coherently. It is about 34 MeV for M_Z and 27 MeV for M_W . The residual difference between working consistently with one or the other definition is about 3 MeV, *i.e.*, of typical size for non-enhanced $\mathcal{O}(\alpha^2)$ corrections [60–62].

Most of the parameters relevant to ν -hadron, ν - e , e -hadron, and e^+e^- processes are determined uniquely and precisely from the data in “model-independent” fits (*i.e.*, fits which allow for an arbitrary electroweak gauge theory). The values for the parameters defined in Eqs. (10.12)–(10.14) are given in Table 10.8 along with the predictions of the SM. The agreement is reasonable, except for the values of g_L^2 and $\epsilon_L(u, d)$, which reflect the discrepancy in the NuTeV results. (The ν -hadron results without the new NuTeV data can be found in the 1998 edition of this *Review*.) The off Z -pole e^+e^- results are difficult to present in a model-independent way because Z -propagator effects are non-negligible at TRISTAN, PETRA, PEP, and LEP 2 energies. However, assuming e - μ - τ universality, the low-energy lepton asymmetries imply [123] $4(g_A^e)^2 = 0.99 \pm 0.05$, in good agreement with the SM prediction $\simeq 1$.

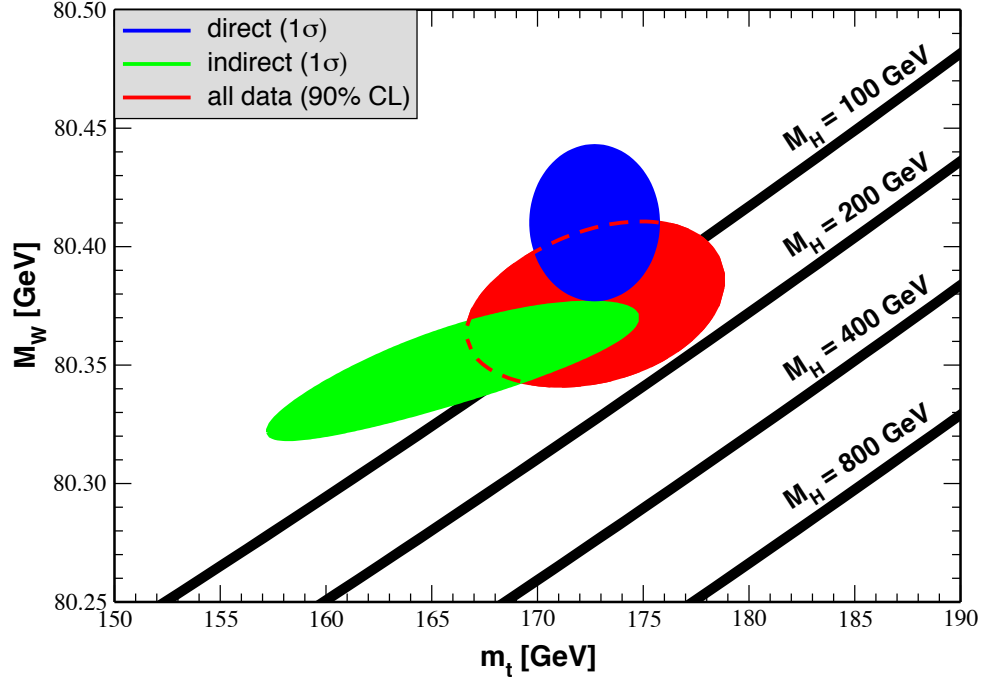


Figure 10.3: One-standard-deviation (39.35%) region in M_W as a function of m_t for the direct and indirect data, and the 90% CL region ($\Delta\chi^2 = 4.605$) allowed by all data. The SM prediction as a function of M_H is also indicated. The widths of the M_H bands reflect the theoretical uncertainty from $\alpha(M_Z)$. See full-color version on color pages at end of book.

10.7. Constraints on new physics

The Z -pole, W -mass, and neutral-current data can be used to search for and set limits on deviations from the SM. In particular, the combination of these indirect data with the direct CDF and $D\bar{O}$ average for m_t allows one to set stringent limits on new physics. We will mainly discuss the effects of exotic particles (with heavy masses $M_{\text{new}} \gg M_Z$ in an expansion in M_Z/M_{new}) on the gauge boson self-energies. (Brief remarks are made on new physics which is not of this type.) Most of the effects on precision measurements can be described by three gauge self-energy parameters S , T , and U . We will define these, as well as related parameters, such as ρ_0 , ϵ_i , and $\hat{\epsilon}_i$, to arise from new physics only. *I.e.*, they are equal to zero ($\rho_0 = 1$) exactly in the SM, and do not include any contributions from m_t or M_H , which are treated separately. Our treatment differs from most of the original papers.

Many extensions of the SM are described by the ρ_0 parameter,

$$\rho_0 \equiv M_W^2 / (M_Z^2 \hat{c}_Z^2 \hat{\rho}), \quad (10.51)$$

which describes new sources of $SU(2)$ breaking that cannot be accounted for by the SM Higgs doublet or m_t effects. In the presence of $\rho_0 \neq 1$, Eq. (10.51) generalizes Eq. (10.8b) while Eq. (10.8a) remains unchanged. Provided that the new physics which yields $\rho_0 \neq 1$ is a small perturbation which does not significantly affect the radiative corrections, ρ_0 can be regarded as a phenomenological parameter which

Table 10.8: Values of the model-independent neutral-current parameters, compared with the SM predictions. There is a second $g_{V,A}^{\nu e}$ solution, given approximately by $g_V^{\nu e} \leftrightarrow g_A^{\nu e}$, which is eliminated by e^+e^- data under the assumption that the neutral current is dominated by the exchange of a single Z . The ϵ_L , as well as the ϵ_R , are strongly correlated and non-Gaussian, so that for implementations we recommend the parametrization using g_i^2 and $\theta_i = \tan^{-1}[\epsilon_i(u)/\epsilon_i(d)]$, $i = L$ or R . In the SM predictions, the uncertainty is from M_Z , M_H , m_t , m_b , m_c , $\hat{\alpha}(M_Z)$, and α_s .

Quantity	Experimental Value	SM	Correlation		
$\epsilon_L(u)$	0.326 ±0.013	0.3459(1)			
$\epsilon_L(d)$	-0.441 ±0.010	-0.4291(1)		non-	
$\epsilon_R(u)$	-0.175 $^{+0.013}_{-0.004}$	-0.1550(1)		Gaussian	
$\epsilon_R(d)$	-0.022 $^{+0.072}_{-0.047}$	0.0776			
g_L^2	0.3005±0.0012	0.3038(2)	-0.11	-0.21	-0.01
g_R^2	0.0311±0.0010	0.0301		-0.02	-0.03
θ_L	2.51 ±0.033	2.4631(1)			0.26
θ_R	4.59 $^{+0.41}_{-0.28}$	5.1765			
$g_V^{\nu e}$	-0.040 ±0.015	-0.0396(3)			-0.05
$g_A^{\nu e}$	-0.507 ±0.014	-0.5064(1)			
$C_{1u} + C_{1d}$	0.147 ±0.004	0.1529(1)	0.95	-0.75	-0.10
$C_{1u} - C_{1d}$	-0.604 ±0.066	-0.5297(4)		-0.79	-0.10
$C_{2u} + C_{2d}$	0.72 ±0.89	-0.0095			-0.11
$C_{2u} - C_{2d}$	-0.071 ±0.044	-0.0621(6)			

multiplies G_F in Eqs. (10.12)–(10.14), (10.29), and Γ_Z in Eq. (10.44). There are enough data to determine ρ_0 , M_H , m_t , and α_s , simultaneously. From the global fit,

$$\rho_0 = 1.0002_{-0.0004}^{+0.0007}, \quad (10.52)$$

$$114.4 \text{ GeV} \leq M_H \leq 191 \text{ GeV}, \quad (10.53)$$

$$m_t = 173.1 \pm 2.9 \text{ GeV}, \quad (10.54)$$

$$\alpha_s(M_Z) = 0.1215 \pm 0.0017, \quad (10.55)$$

where the lower limit on M_H is the direct search bound. (If the direct limit is ignored one obtains $M_H = 66_{-30}^{+85}$ GeV and $\rho_0 = 0.9996_{-0.0007}^{+0.0010}$.) The error bar in Eq. (10.52) is highly asymmetric: at the 2σ level one has $\rho_0 = 1.0002_{-0.0009}^{+0.0024}$ and $M_H \leq 654$ GeV. Clearly, in

the presence of ρ_0 upper limits on M_H become much weaker. The result in Eq. (10.52) is in remarkable agreement with the SM expectation, $\rho_0 = 1$. It can be used to constrain higher-dimensional Higgs representations to have vacuum expectation values of less than a few percent of those of the doublets. Indeed, the relation between M_W and M_Z is modified if there are Higgs multiplets with weak isospin $> 1/2$ with significant vacuum expectation values. In order to calculate to higher orders in such theories one must define a set of four fundamental renormalized parameters which one may conveniently choose to be α , G_F , M_Z , and M_W , since M_W and M_Z are directly measurable. Then \hat{s}_Z^2 and ρ_0 can be considered dependent parameters.

Eq. (10.52) can also be used to constrain other types of new physics. For example, non-degenerate multiplets of heavy fermions or scalars break the vector part of weak SU(2) and lead to a decrease in the value of M_Z/M_W . A non-degenerate SU(2) doublet $\begin{pmatrix} f_1 \\ f_2 \end{pmatrix}$ yields a positive contribution to ρ_0 [191] of

$$\frac{CG_F}{8\sqrt{2}\pi^2} \Delta m^2, \quad (10.56)$$

where

$$\Delta m^2 \equiv m_1^2 + m_2^2 - \frac{4m_1^2 m_2^2}{m_1^2 - m_2^2} \ln \frac{m_1}{m_2} \geq (m_1 - m_2)^2, \quad (10.57)$$

and $C = 1$ (3) for color singlets (triplets). Thus, in the presence of such multiplets, one has

$$\frac{3G_F}{8\sqrt{2}\pi^2} \sum_i \frac{C_i}{3} \Delta m_i^2 = \rho_0 - 1, \quad (10.58)$$

where the sum includes fourth-family quark or lepton doublets, $\begin{pmatrix} t' \\ b' \end{pmatrix}$ or $\begin{pmatrix} E^0 \\ E^- \end{pmatrix}$, and scalar doublets such as $\begin{pmatrix} \tilde{t} \\ \tilde{b} \end{pmatrix}$ in Supersymmetry (in the absence of $L - R$ mixing). This implies

$$\sum_i \frac{C_i}{3} \Delta m_i^2 \leq (90 \text{ GeV})^2 \quad (10.59)$$

at 95% CL. The corresponding constraints on non-degenerate squark and slepton doublets are even stronger, $\sum_i C_i \Delta m_i^2 / 3 \leq (64 \text{ GeV})^2$. This is due to the supersymmetric Higgs mass bound, $m_{h^0} < 150 \text{ GeV}$, and the very strong correlation between m_{h^0} and ρ_0 (84%).

Non-degenerate multiplets usually imply $\rho_0 > 1$. Similarly, heavy Z' bosons decrease the prediction for M_Z due to mixing and generally lead to $\rho_0 > 1$ [192]. On the other hand, additional Higgs doublets which participate in spontaneous symmetry breaking [193], heavy lepton doublets involving Majorana neutrinos [194], and the vacuum expectation values of Higgs triplets or higher-dimensional representations can contribute to ρ_0 with either sign. Allowing for the presence of heavy degenerate chiral multiplets (the S parameter, to be discussed below) affects the determination of ρ_0 from the data, at present leading to a smaller value (for fixed M_H).

34 10. Electroweak model and constraints on new physics

A number of authors [195–200] have considered the general effects on neutral-current and Z and W -boson observables of various types of heavy (*i.e.*, $M_{\text{new}} \gg M_Z$) physics which contribute to the W and Z self-energies but which do not have any direct coupling to the ordinary fermions. In addition to non-degenerate multiplets, which break the vector part of weak SU(2), these include heavy degenerate multiplets of chiral fermions which break the axial generators. The effects of one degenerate chiral doublet are small, but in Technicolor theories there may be many chiral doublets and therefore significant effects [195].

Such effects can be described by just three parameters, S , T , and U at the (electroweak) one-loop level. (Three additional parameters are needed if the new physics scale is comparable to M_Z [201]. Further generalizations, including effects relevant to LEP 2, are described in Ref. 202.) T is proportional to the difference between the W and Z self-energies at $Q^2 = 0$ (*i.e.*, vector SU(2)-breaking), while S ($S + U$) is associated with the difference between the Z (W) self-energy at $Q^2 = M_{Z,W}^2$ and $Q^2 = 0$ (axial SU(2)-breaking). Denoting the contributions of new physics to the various self-energies by Π_{ij}^{new} , we have

$$\hat{\alpha}(M_Z)T \equiv \frac{\Pi_{WW}^{\text{new}}(0)}{M_W^2} - \frac{\Pi_{ZZ}^{\text{new}}(0)}{M_Z^2}, \quad (10.60a)$$

$$\begin{aligned} \frac{\hat{\alpha}(M_Z)}{4\hat{s}_Z^2\hat{c}_Z^2}S &\equiv \frac{\Pi_{ZZ}^{\text{new}}(M_Z^2) - \Pi_{ZZ}^{\text{new}}(0)}{M_Z^2} \\ &- \frac{\hat{c}_Z^2 - \hat{s}_Z^2}{\hat{c}_Z\hat{s}_Z} \frac{\Pi_{Z\gamma}^{\text{new}}(M_Z^2)}{M_Z^2} - \frac{\Pi_{\gamma\gamma}^{\text{new}}(M_Z^2)}{M_Z^2}, \end{aligned} \quad (10.60b)$$

$$\begin{aligned} \frac{\hat{\alpha}(M_Z)}{4\hat{s}_Z^2}(S + U) &\equiv \frac{\Pi_{WW}^{\text{new}}(M_W^2) - \Pi_{WW}^{\text{new}}(0)}{M_W^2} \\ &- \frac{\hat{c}_Z}{\hat{s}_Z} \frac{\Pi_{Z\gamma}^{\text{new}}(M_Z^2)}{M_Z^2} - \frac{\Pi_{\gamma\gamma}^{\text{new}}(M_Z^2)}{M_Z^2}. \end{aligned} \quad (10.60c)$$

S , T , and U are defined with a factor proportional to $\hat{\alpha}$ removed, so that they are expected to be of order unity in the presence of new physics. In the $\overline{\text{MS}}$ scheme as defined in Ref. 52, the last two terms in Eq. (10.60b) and Eq. (10.60c) can be omitted (as was done in some earlier editions of this *Review*). These three parameters are related to other parameters (S_i , h_i , $\hat{\epsilon}_i$) defined in Refs. [52,196,197] by

$$\begin{aligned} T &= h_V = \hat{\epsilon}_1/\alpha, \\ S &= h_{AZ} = S_Z = 4\hat{s}_Z^2\hat{\epsilon}_3/\alpha, \\ U &= h_{AW} - h_{AZ} = S_W - S_Z = -4\hat{s}_Z^2\hat{\epsilon}_2/\alpha. \end{aligned} \quad (10.61)$$

A heavy non-degenerate multiplet of fermions or scalars contributes positively to T as

$$\rho_0 - 1 = \frac{1}{1 - \alpha T} - 1 \simeq \alpha T, \quad (10.62)$$

where ρ_0 is given in Eq. (10.58). The effects of non-standard Higgs representations cannot be separated from heavy non-degenerate multiplets unless the new physics has other consequences, such as vertex corrections. Most of the original papers defined T to include the effects of loops only. However, we will redefine T to include all new sources of SU(2) breaking, including non-standard Higgs, so that T and ρ_0 are equivalent by Eq. (10.62).

A multiplet of heavy degenerate chiral fermions yields

$$S = C \sum_i \left(t_{3L}(i) - t_{3R}(i) \right)^2 / 3\pi , \quad (10.63)$$

where $t_{3L,R}(i)$ is the third component of weak isospin of the left-(right-)handed component of fermion i and C is the number of colors. For example, a heavy degenerate ordinary or mirror family would contribute $2/3\pi$ to S . In Technicolor models with QCD-like dynamics, one expects [195] $S \sim 0.45$ for an iso-doublet of techni-fermions, assuming $N_{TC} = 4$ techni-colors, while $S \sim 1.62$ for a full techni-generation with $N_{TC} = 4$; T is harder to estimate because it is model dependent. In these examples one has $S \geq 0$. However, the QCD-like models are excluded on other grounds (flavor changing neutral-currents, and too-light quarks and pseudo-Goldstone bosons [203]). In particular, these estimates do not apply to models of walking Technicolor [203], for which S can be smaller or even negative [204]. Other situations in which $S < 0$, such as loops involving scalars or Majorana particles, are also possible [205]. The simplest origin of $S < 0$ would probably be an additional heavy Z' boson [192], which could mimic $S < 0$. Supersymmetric extensions of the SM generally give very small effects. See Refs. 155,206 and the Section on Supersymmetry in this *Review* for a complete set of references.

Most simple types of new physics yield $U = 0$, although there are counter-examples, such as the effects of anomalous triple gauge vertices [197].

The SM expressions for observables are replaced by

$$\begin{aligned} M_Z^2 &= M_{Z0}^2 \frac{1 - \alpha T}{1 - G_F M_{Z0}^2 S / 2\sqrt{2}\pi} , \\ M_W^2 &= M_{W0}^2 \frac{1}{1 - G_F M_{W0}^2 (S + U) / 2\sqrt{2}\pi} , \end{aligned} \quad (10.64)$$

where M_{Z0} and M_{W0} are the SM expressions (as functions of m_t and M_H) in the $\overline{\text{MS}}$ scheme. Furthermore,

$$\begin{aligned} \Gamma_Z &= \frac{1}{1 - \alpha T} M_Z^3 \beta_Z , \\ \Gamma_W &= M_W^3 \beta_W , \\ A_i &= \frac{1}{1 - \alpha T} A_{i0} , \end{aligned} \quad (10.65)$$

where β_Z and β_W are the SM expressions for the reduced widths Γ_{Z0}/M_{Z0}^3 and Γ_{W0}/M_{W0}^3 , M_Z and M_W are the physical masses, and A_i (A_{i0}) is a neutral-current amplitude (in the SM).

36 10. Electroweak model and constraints on new physics

The data allow a simultaneous determination of \hat{s}_Z^2 (from the Z -pole asymmetries), S (from M_Z), U (from M_W), T (mainly from Γ_Z), α_s (from R_ℓ , σ_{had} , and τ_τ), and m_t (from CDF and DØ), with little correlation among the SM parameters:

$$\begin{aligned} S &= -0.13 \pm 0.10 \text{ } (-0.08) \text{ ,} \\ T &= -0.13 \pm 0.11 \text{ } (+0.09) \text{ ,} \\ U &= 0.20 \pm 0.12 \text{ } (+0.01) \text{ ,} \end{aligned} \tag{10.66}$$

and $\hat{s}_Z^2 = 0.23124 \pm 0.00016$, $\alpha_s(M_Z) = 0.1223 \pm 0.0018$, $m_t = 172.6 \pm 2.9$ GeV, where the uncertainties are from the inputs. The central values assume $M_H = 117$ GeV, and in parentheses we show the change for $M_H = 300$ GeV. As can be seen, the SM parameters (U) can be determined with no (little) M_H dependence. On the other hand, S , T , and M_H cannot be obtained simultaneously, because the Higgs boson loops themselves are resembled approximately by oblique effects. Eqs. (10.66) show that negative (positive) contributions to the S (T) parameter can weaken or entirely remove the strong constraints on M_H from the SM fits. Specific models in which a large M_H is compensated by new physics are reviewed in Ref. 207. The parameters in Eqs. (10.66), which by definition are due to new physics only, all deviate by more than one standard deviation from the SM values of zero. However, these deviations are correlated. Fixing $U = 0$ (as is done in Fig. 10.4) will also move S and T to values compatible with zero within errors,

$$\begin{aligned} S &= -0.07 \pm 0.09 \text{ } (-0.07) \text{ ,} \\ T &= -0.03 \pm 0.09 \text{ } (+0.09) \text{ .} \end{aligned} \tag{10.67}$$

Using Eq. (10.62) the value of ρ_0 corresponding to T is 0.9990 ± 0.0009 (+0.0007), while the one corresponding to Eq. (10.67) is 0.9997 ± 0.0007 (+0.0007). The values of the $\hat{\epsilon}$ parameters defined in Eq. (10.61) are

$$\begin{aligned} \hat{\epsilon}_3 &= -0.0011 \pm 0.0008 \text{ } (-0.0006) \text{ ,} \\ \hat{\epsilon}_1 &= -0.0010 \pm 0.0009 \text{ } (+0.0007) \text{ ,} \\ \hat{\epsilon}_2 &= -0.0017 \pm 0.0010 \text{ } (-0.0001) \text{ .} \end{aligned} \tag{10.68}$$

Unlike the original definition, we defined the quantities in Eqs. (10.68) to vanish identically in the absence of new physics and to correspond directly to the parameters S , T , and U in Eqs. (10.66). There is a strong correlation (84%) between the S and T parameters. The allowed region in $S - T$ is shown in Fig. 10.4. From Eqs. (10.66) one obtains $S \leq 0.03$ (-0.04) and $T \leq 0.06$ (0.14) at 95% CL for $M_H = 117$ GeV (300 GeV). If one fixes $M_H = 600$ GeV and requires the constraint $S \geq 0$ (as is appropriate in QCD-like Technicolor models) then $S \leq 0.09$ (Bayesian) or $S \leq 0.06$ (frequentist). This rules out simple Technicolor models with many techni-doublets and QCD-like dynamics.

An extra generation of ordinary fermions is excluded at the 99.999% CL on the basis of the S parameter alone, corresponding to $N_F = 2.81 \pm 0.24$ for the number of families. This result assumes that there are no new contributions to T or U and therefore that any new families are degenerate. In principle this restriction can be relaxed by allowing

T to vary as well, since $T > 0$ is expected from a non-degenerate extra family. However, the data currently favor $T < 0$, thus strengthening the exclusion limits. A more detailed analysis is required if the extra neutrino (or the extra down-type quark) is close to its direct mass limit [208]. This can drive S to small or even negative values but at the expense of too-large contributions to T . These results are in agreement with a fit to the number of light neutrinos, $N_\nu = 2.986 \pm 0.007$ (which favors a larger value for $\alpha_s(M_Z) = 0.1231 \pm 0.0020$ mainly from R_ℓ and τ_τ). However, the S parameter fits are valid even for a very heavy fourth family neutrino.

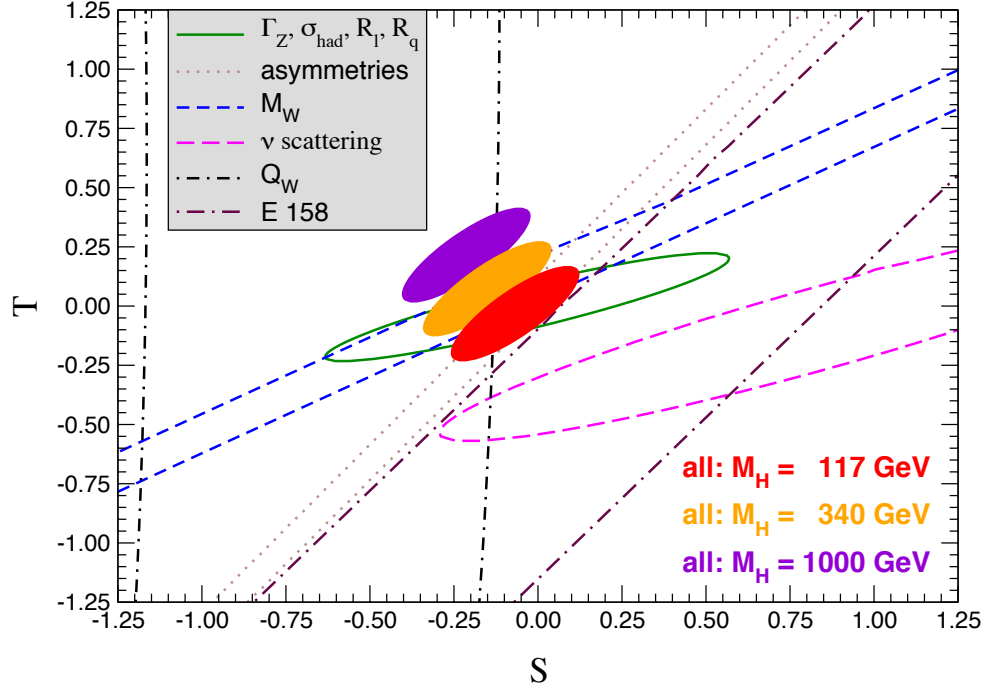


Figure 10.4: 1σ constraints (39.35 %) on S and T from various inputs combined with M_Z . S and T represent the contributions of new physics only. (Uncertainties from m_t are included in the errors.) The contours assume $M_H = 117$ GeV except for the central and upper 90% CL contours allowed by all data, which are for $M_H = 340$ GeV and 1000 GeV, respectively. Data sets not involving M_W are insensitive to U . Due to higher order effects, however, $U = 0$ has to be assumed in all fits. α_s is constrained using the τ lifetime as additional input in all fits. See full-color version on color pages at end of book.

There is no simple parametrization that is powerful enough to describe the effects of every type of new physics on every possible observable. The S , T , and U formalism describes many types of heavy physics which affect only the gauge self-energies, and it can be applied to all precision observables. However, new physics which couples directly to ordinary fermions, such as heavy Z' bosons [192] or mixing with exotic fermions [209] cannot be fully parametrized in the S , T , and U framework. It is convenient to treat these types of new physics by parameterizations that are specialized to that particular class of

38 10. Electroweak model and constraints on new physics

theories (*e.g.*, extra Z' bosons), or to consider specific models (which might contain, *e.g.*, Z' bosons and exotic fermions with correlated parameters). Constraints on various types of new physics are reviewed in Refs. [47,116,210,211].

Fits to Supersymmetric models are described in Refs. 155 and 212. Models involving strong dynamics (such as (extended) Technicolor) for electroweak breaking are considered in Ref. 213. The effects of compactified extra spatial dimensions at the TeV scale are reviewed in Ref. 214, and constraints on Little Higgs models in Ref. 215. Limits on new four-Fermi operators and on leptoquarks using LEP 2 and lower energy data are given in Ref. 130.

An alternate formalism [216] defines parameters, $\epsilon_1, \epsilon_2, \epsilon_3, \epsilon_b$ in terms of the specific observables $M_W/M_Z, \Gamma_{\ell\ell}, A_{FB}^{(0,\ell)}$, and R_b . The definitions coincide with those for $\hat{\epsilon}_i$ in Eqs. (10.60) and (10.61) for physics which affects gauge self-energies only, but the ϵ 's now parametrize arbitrary types of new physics. However, the ϵ 's are not related to other observables unless additional model dependent assumptions are made. Another approach [217–219] parametrizes new physics in terms of gauge-invariant sets of operators. It is especially powerful in studying the effects of new physics on non-Abelian gauge vertices. The most general approach introduces deviation vectors [210]. Each type of new physics defines a deviation vector, the components of which are the deviations of each observable from its SM prediction, normalized to the experimental uncertainty. The length (direction) of the vector represents the strength (type) of new physics.

Table 10.9: 95% CL lower mass limits (in GeV) from low energy and Z pole data on various extra Z' gauge bosons, appearing in models of unification and string theory. (More general parametrizations are described in [224]). ρ_0 free indicates a completely arbitrary Higgs sector, while $\rho_0 = 1$ restricts to Higgs doublets and singlets with still unspecified charges. The CDF bounds from searches for $\bar{p}p \rightarrow e^+e^-, \mu^+\mu^-$ [225] and the LEP 2 $e^+e^- \rightarrow f\bar{f}$ [133] bounds are listed in the last two columns, respectively. (The CDF bounds would be weakened if there are open supersymmetric or exotic decay channels [226].)

Z'	ρ_0 free	$\rho_0 = 1$	CDF (direct)	LEP 2
Z_χ	551	545	720	673
Z_ψ	151	146	690	481
Z_η	379	365	715	434
Z_{LR}	570	564	630	804
Z_{SM}	822	809	845	1787
Z_{string}	582	578	–	–

One of the best motivated kinds of physics beyond the SM besides Supersymmetry are extra Z' bosons [220]. They do not spoil the observed approximate gauge coupling unification, and appear copiously in many Grand Unified Theories (GUTs), most Superstring models [221], as well as in dynamical symmetry breaking [213,222] and Little

Higgs models [215]. For example, the SO(10) GUT contains an extra U(1) as can be seen from its maximal subgroup, $SU(5) \times U(1)_\chi$. Similarly, the E₆ GUT contains the subgroup $SO(10) \times U(1)_\psi$. The Z_ψ possesses only axial-vector couplings to the ordinary fermions, and its mass is generally less constrained. The Z_η boson is the linear combination $\sqrt{3/8}Z_\chi - \sqrt{5/8}Z_\psi$. The Z_{LR} boson occurs in left-right models with gauge group $SU(3)_C \times SU(2)_L \times SU(2)_R \times U(1)_{B-L} \subset SO(10)$. The sequential Z_{SM} boson is defined to have the same couplings to fermions as the SM Z -boson. Such a boson is not expected in the context of gauge theories unless it has different couplings to exotic fermions than the ordinary Z . However, it serves as a useful reference case when comparing constraints from various sources. It could also play the role of an excited state of the ordinary Z in models with extra dimensions at the weak scale [214]. Finally, we consider a Superstring motivated Z_{string} boson appearing in a specific model [223]. The potential Z' boson is in general a superposition of the SM Z and the new boson associated with the extra U(1). The mixing angle θ satisfies,

$$\tan^2 \theta = \frac{M_{Z_1^0}^2 - M_Z^2}{M_{Z'}^2 - M_{Z_1^0}^2},$$

where $M_{Z_1^0}$ is the SM value for M_Z in the absence of mixing. Note, that $M_Z < M_{Z_1^0}$, and that the SM Z couplings are changed by the mixing. If the Higgs U(1)' quantum numbers are known, there will be an extra constraint,

$$\theta = C \frac{g_2}{g_1} \frac{M_Z^2}{M_{Z'}^2}, \quad (10.69)$$

where $g_{1,2}$ are the U(1) and U(1)' gauge couplings with $g_2 = \sqrt{5/3} \sin \theta_W \sqrt{\lambda} g_1$ and $g_1 = \sqrt{g^2 + g'^2}$. $\lambda \sim 1$ (which we assume) if the GUT group breaks directly to $SU(3) \times SU(2) \times U(1) \times U(1)'$. C is a function of vacuum expectation values. For minimal Higgs sectors it can be found in Ref. 192. Table 10.9 shows the 95% CL lower mass limits obtained from a somewhat earlier data set [227] for ρ_0 free and $\rho_0 = 1$, respectively. In cases of specific minimal Higgs sectors where C is known, the Z' mass limits are generally pushed into the TeV region. The limits on $|\theta|$ are typically $< \text{few} \times 10^{-3}$. For more details see [227,228] and the Section on ‘‘The Z' Searches’’ in this *Review*. Also listed in Table 10.9 are the direct lower limits on Z' production from CDF [225] and LEP 2 bounds [45]. The final LEP 1 value for σ_{had} , some previous values for $Q_W(\text{Cs})$, NuTeV, and $A_{FB}^{0,b}$ (for family-nonuniversal couplings [229]) modify the results and might even suggest the possible existence of a Z' [184,230].

Acknowledgments:

This work was supported in part by CONACyT (Mexico) contract 42026–F, by DGAPA–UNAM contract PAPIIT IN112902, and by the U.S. Department of Energy under Grant No. DOE-EY-76-02-3071.

References:

1. S. Weinberg, Phys. Rev. Lett. **19**, 1264 (1967);
A. Salam, p. 367 of *Elementary Particle Theory*, ed. N. Svartholm (Almquist and Wiksells, Stockholm, 1969);
S.L. Glashow, J. Iliopoulos, and L. Maiani, Phys. Rev. **D2**, 1285 (1970).
2. J.L. Rosner, hep-ph/0410281;
CKMfitter Group: J. Charles *et al.*, Eur. Phys. J. **C41**, 1 (2005).
3. For reviews, see G. Barbiellini and C. Santoni, Riv. Nuovo Cimento **9(2)**, 1 (1986);
E.D. Commins and P.H. Bucksbaum, *Weak Interactions of Leptons and Quarks*, (Cambridge Univ. Press, Cambridge, 1983);
W. Fetscher and H.J. Gerber, p. 657 of Ref. 4;
J. Deutsch and P. Quin, p. 706 of Ref. 4;
J.M. Conrad, M.H. Shaevitz, and T. Bolton, Rev. Mod. Phys. **70**, 1341 (1998).
4. *Precision Tests of the Standard Electroweak Model*, ed. P. Langacker (*World Scientific, Singapore, 1995*).
5. J. Erler and M. Luo, Phys. Lett. **B558**, 125 (2003).
6. CDF, DØ, and the Tevatron Electroweak Working Group: J.F. Arguin *et al.*, hep-ex/0507091.
7. CDF: T. Affolder *et al.*, Phys. Rev. **D63**, 032003 (2001).
8. DØ: B. Abbott *et al.*, Phys. Rev. **D60**, 052001 (1999);
DØ: V.M. Abazov *et al.*, Nature **429**, 638 (2004);
DØ: V.M. Abazov *et al.*, Phys. Lett. **B606**, 25 (2005).
9. K. Melnikov and T. v. Ritbergen, Phys. Lett. **B482**, 99 (2000).
10. S.J. Brodsky, G.P. Lepage, and P.B. Mackenzie, Phys. Rev. **D28**, 228 (1983).
11. N. Gray *et al.*, Z. Phys. **C48**, 673 (1990).
12. For reviews, see the article on “The Higgs boson” in this *Review*;
J. Gunion, H.E. Haber, G.L. Kane, and S. Dawson, *The Higgs Hunter’s Guide*, (Addison-Wesley, Redwood City, 1990);
M. Sher, Phys. Reports **179**, 273 (1989);
M. Carena and H.E. Haber, Prog. Part. Nucl. Phys. **50**, 63 (2003);
L. Reina, hep-ph/0512377.
13. P.J. Mohr and B.N. Taylor, Rev. Mod. Phys. **72**, 351 (2000).
14. TOPAZ: I. Levine *et al.*, Phys. Rev. Lett. **78**, 424 (1997);
VENUS: S. Okada *et al.*, Phys. Rev. Lett. **81**, 2428 (1998);
L3: M. Acciarri *et al.*, Phys. Lett. **B476**, 40 (2000);
L3: P. Achard *et al.*, Phys. Lett. **B623**, 26 (2005);
OPAL: G. Abbiendi *et al.*, Eur. Phys. J. **C33**, 173 (2004);
OPAL: G. Abbiendi *et al.*, Eur. Phys. J. **C45**, 1 (2006).
15. S. Fanchiotti, B. Kniehl, and A. Sirlin, Phys. Rev. **D48**, 307 (1993) and references therein.
16. J. Erler, Phys. Rev. **D59**, 054008 (1999).
17. CMD 2: R.R. Akhmetshin *et al.*, Phys. Lett. **B578**, 285 (2004).
18. M. Davier, S. Eidelman, A. Höcker, and Z. Zhang, Eur. Phys. J. **C31**, 503 (2003).
19. ALEPH: S. Schael *et al.*, Phys. Reports **421**, 191 (2005).

20. M. Davier, A. Höcker and Z. Zhang, hep-ph/0507078.
21. A.D. Martin and D. Zeppenfeld, Phys. Lett. **B345**, 558 (1995).
22. S. Eidelman and F. Jegerlehner, Z. Phys. **C67**, 585 (1995).
23. B.V. Geshkenbein and V.L. Morgunov, Phys. Lett. **B340**, 185 (1995);
B.V. Geshkenbein and V.L. Morgunov, Phys. Lett. **B352**, 456 (1995).
24. H. Burkhardt and B. Pietrzyk, Phys. Lett. **B356**, 398 (1995).
25. M.L. Swartz, Phys. Rev. **D53**, 5268 (1996).
26. R. Alemany, M. Davier, and A. Höcker, Eur. Phys. J. **C2**, 123 (1998).
27. N.V. Krasnikov and R. Rodenberg, Nuovo Cimento **111A**, 217 (1998).
28. M. Davier and A. Höcker, Phys. Lett. **B419**, 419 (1998).
29. J.H. Kühn and M. Steinhauser, Phys. Lett. **B437**, 425 (1998).
30. M. Davier and A. Höcker, Phys. Lett. **B435**, 427 (1998).
31. S. Groote, J.G. Körner, K. Schilcher, N.F. Nasrallah, Phys. Lett. **B440**, 375 (1998).
32. A.D. Martin, J. Outhwaite, and M.G. Ryskin, Phys. Lett. **B492**, 69 (2000).
33. H. Burkhardt and B. Pietrzyk, Phys. Lett. **B513**, 46 (2001).
34. J.F. de Troconiz and F.J. Yndurain, Phys. Rev. **D65**, 093002 (2002).
35. F. Jegerlehner, Nucl. Phys. Proc. Suppl. **126**, 325 (2004).
36. K. Hagiwara, A. D. Martin, D. Nomura and T. Teubner, Phys. Rev. **D69**, 093003 (2004).
37. H. Burkhardt and B. Pietrzyk, Phys. Rev. **D72**, 057501 (2005).
38. BES: J.Z. Bai *et al.*, Phys. Rev. Lett. **88**, 101802 (2002);
G.S. Huang, hep-ex/0105074.
39. SND: M.N. Achasov *et al.*, hep-ex/0506076.
40. CMD and OLYA: L.M. Barkov *et al.*, Nucl. Phys. **B256**, 365 (1985).
41. S. Binner, J.H. Kühn, and K. Melnikov, Phys. Lett. **B459**, 279 (1999).
42. KLOE: A. Aloisio *et al.*, Phys. Lett. **B606**, 12 (2005).
43. W.J. Marciano and A. Sirlin, Phys. Rev. Lett. **61**, 1815 (1988).
44. T. van Ritbergen and R.G. Stuart, Phys. Rev. Lett. **82**, 488 (1999).
45. ALEPH, DELPHI, L3, OPAL, SLD, LEP Electroweak Working Group, SLD
Electroweak and Heavy Flavour Groups: S. Schael *et al.*, hep-ex/0509008.
46. Earlier analyses include U. Amaldi *et al.*, Phys. Rev. **D36**, 1385 (1987);
G. Costa *et al.*, Nucl. Phys. **B297**, 244 (1988);
Deep inelastic scattering is considered by G.L. Fogli and D. Haidt, Z. Phys. **C40**,
379 (1988);
P. Langacker and M. Luo, Phys. Rev. **D44**, 817 (1991);
For more recent analyses, see Ref. 47.
47. P. Langacker, p. 883 of Ref. 4;
J. Erler and P. Langacker, Phys. Rev. **D52**, 441 (1995).
48. J. Erler and M.J. Ramsey-Musolf, Prog. Part. Nucl. Phys. **54**, 351 (2005);
Neutrino scattering is reviewed by J.M. Conrad *et al.* in Ref. 3;
Nonstandard neutrino interactions are surveyed in Z. Berezhiani and A. Rossi, Phys.
Lett. **B535**, 207 (2002);
S. Davidson, C. Peña-Garay, N. Rius, and A. Santamaria, JHEP **0303**, 011 (2003).

42 10. Electroweak model and constraints on new physics

49. A. Sirlin, Phys. Rev. **D22**, 971 (1980);
A. Sirlin, Phys. Rev. **D29**, 89 (1984);
D.C. Kennedy *et al.*, Nucl. Phys. **B321**, 83 (1989);
D.C. Kennedy and B.W. Lynn, Nucl. Phys. **B322**, 1 (1989);
D.Yu. Bardin *et al.*, Z. Phys. **C44**, 493 (1989);
W. Hollik, Fortsch. Phys. **38**, 165 (1990);
For reviews, see the articles by W. Hollik, pp. 37 and 117, and W. Marciano, p. 170 in Ref. 4. Extensive references to other papers are given in Ref. 46.
50. V.A. Novikov, L.B. Okun, and M.I. Vysotsky, Nucl. Phys. **B397**, 35 (1993).
51. W. Hollik in Ref. 49 and references therein.
52. W.J. Marciano and J.L. Rosner, Phys. Rev. Lett. **65**, 2963 (1990).
53. G. Degrassi, S. Fanchiotti, and A. Sirlin, Nucl. Phys. **B351**, 49 (1991).
54. G. Degrassi and A. Sirlin, Nucl. Phys. **B352**, 342 (1991).
55. P. Gambino and A. Sirlin, Phys. Rev. **D49**, 1160 (1994).
56. ZFITTER: D. Bardin *et al.*, Comput. Phys. Commun. **133**, 229 (2001) and references therein;
ZFITTER: A.B. Arbuzov *et al.*, hep-ph/0507146.
57. R. Barbieri *et al.*, Phys. Lett. **B288**, 95 (1992) and *ibid.* **312**, 511(E) (1993);
R. Barbieri *et al.*, Nucl. Phys. **B409**, 105 (1993).
58. J. Fleischer, O.V. Tarasov, and F. Jegerlehner, Phys. Lett. **B319**, 249 (1993).
59. G. Degrassi, P. Gambino, and A. Vicini, Phys. Lett. **B383**, 219 (1996);
G. Degrassi, P. Gambino, and A. Sirlin, Phys. Lett. **B394**, 188 (1997).
60. A. Freitas, W. Hollik, W. Walter, and G. Weiglein, Phys. Lett. **B495**, 338 (2000) and *ibid.* **570**, 260(E) (2003);
M. Awramik and M. Czakon, Phys. Lett. **B568**, 48 (2003).
61. A. Freitas, W. Hollik, W. Walter, and G. Weiglein, Nucl. Phys. **B632**, 189 (2002) and *ibid.* **666**, 305(E) (2003);
M. Awramik and M. Czakon, Phys. Rev. Lett. **89**, 241801 (2002);
A. Onishchenko and O. Veretin, Phys. Lett. **B551**, 111 (2003).
62. M. Awramik, M. Czakon, A. Freitas and G. Weiglein, Phys. Rev. Lett. **93**, 201805 (2004);
W. Hollik, U. Meier and S. Uccirati, Nucl. Phys. **B731**, 213 (2005).
63. A. Djouadi and C. Verzegnassi, Phys. Lett. **B195**, 265 (1987);
A. Djouadi, Nuovo Cimento **100A**, 357 (1988).
64. K.G. Chetyrkin, J.H. Kühn, and M. Steinhauser, Phys. Lett. **B351**, 331 (1995);
L. Avdeev *et al.*, Phys. Lett. **B336**, 560 (1994) and **B349**, 597(E) (1995).
65. B.A. Kniehl, J.H. Kühn, and R.G. Stuart, Phys. Lett. **B214**, 621 (1988);
B.A. Kniehl, Nucl. Phys. **B347**, 86 (1990);
F. Halzen and B.A. Kniehl, Nucl. Phys. **B353**, 567 (1991);
A. Djouadi and P. Gambino, Phys. Rev. **D49**, 4705 (1994);
A. Djouadi and P. Gambino, Phys. Rev. **D49**, 3499 (1994) and *ibid.* **53**, 4111(E) (1996).
66. K.G. Chetyrkin, J.H. Kühn, and M. Steinhauser, Phys. Rev. Lett. **75**, 3394 (1995).
67. J.J. van der Bij *et al.*, Phys. Lett. **B498**, 156 (2001).

68. M. Faisst, J.H. Kühn, T. Seidensticker, and O. Veretin, Nucl. Phys. **B665**, 649 (2003).
69. R. Boughezal, J.B. Tausk, and J.J. van der Bij, Nucl. Phys. **B713**, 278 (2005);
R. Boughezal, J.B. Tausk, and J.J. van der Bij, Nucl. Phys. **B725**, 3 (2005).
70. J. Fleischer *et al.*, Phys. Lett. **B293**, 437 (1992);
K.G. Chetyrkin, A. Kwiatkowski, and M. Steinhauser, Mod. Phys. Lett. **A8**, 2785 (1993).
71. R. Harlander, T. Seidensticker, and M. Steinhauser, Phys. Lett. **B426**, 125 (1998);
J. Fleischer *et al.*, Phys. Lett. **B459**, 625 (1999).
72. A. Czarnecki and J.H. Kühn, Phys. Rev. Lett. **77**, 3955 (1996).
73. J. Erler, hep-ph/0005084.
74. For reviews, see F. Perrier, p. 385 of Ref. 4;
J.M. Conrad *et al.* in Ref. 3.
75. CDHS: H. Abramowicz *et al.*, Phys. Rev. Lett. **57**, 298 (1986);
CDHS: A. Blondel *et al.*, Z. Phys. **C45**, 361 (1990).
76. CHARM: J.V. Allaby *et al.*, Phys. Lett. **B177**, 446 (1986);
CHARM: J.V. Allaby *et al.*, Z. Phys. **C36**, 611 (1987).
77. CCFR: C.G. Arroyo *et al.*, Phys. Rev. Lett. **72**, 3452 (1994);
CCFR: K.S. McFarland *et al.*, Eur. Phys. J. **C1**, 509 (1998).
78. NOMAD: R. Petti *et al.*, hep-ex/0411032.
79. R.M. Barnett, Phys. Rev. **D14**, 70 (1976);
H. Georgi and H.D. Politzer, Phys. Rev. **D14**, 1829 (1976).
80. LAB-E: S.A. Rabinowitz *et al.*, Phys. Rev. Lett. **70**, 134 (1993).
81. E.A. Paschos and L. Wolfenstein, Phys. Rev. **D7**, 91 (1973).
82. NuTeV: G. P. Zeller *et al.*, Phys. Rev. Lett. **88**, 091802 (2002).
83. For reviews including discussions of possible new physics explanations, see
S. Davidson *et al.*, JHEP **0202**, 037 (2002);
J.T. Londergan, Nucl. Phys. Proc. Suppl. **141**, 68 (2005).
84. J. Alwall and G. Ingelman, Phys. Rev. **D70**, 111505 (2004);
Y. Ding, R.G. Xu and B.Q. Ma, Phys. Lett. **B607**, 101 (2005);
M. Wakamatsu, Phys. Rev. **D71**, 057504 (2005);
M. Glück, P. Jimenez-Delgado, and E. Reya, Phys. Rev. Lett. **95**, 022002 (2005).
85. NuTeV: M. Goncharov *et al.*, Phys. Rev. **D64**, 112006 (2001);
NuTeV: D. Mason *et al.*, hep-ex/0405037.
86. NuTeV: G.P. Zeller *et al.*, Phys. Rev. **D65**, 111103 (2002);
NuTeV: R. H. Bernstein *et al.*, J. Phys. G **29**, 1919 (2003).
87. S. Kretzer *et al.*, Phys. Rev. Lett. **93**, 041802 (2004).
88. E. Sather, Phys. Lett. **B274**, 433 (1992);
E.N. Rodionov, A.W. Thomas, and J.T. Londergan, Mod. Phys. Lett. **A9**, 1799 (1994).
89. A.D. Martin, R.G. Roberts, W.J. Stirling and R.S. Thorne, Eur. Phys. J. **C35**, 325 (2004).

44 10. Electroweak model and constraints on new physics

90. S. Kumano, Phys. Rev. **D66**, 111301 (2002);
S.A. Kulagin, Phys. Rev. **D67**, 091301 (2003);
M. Hirai, S. Kumano and T. H. Nagai, Phys. Rev. **D71**, 113007 (2005).
91. G.A. Miller and A.W. Thomas, Int. J. Mod. Phys. A **20**, 95 (2005).
92. S.J. Brodsky, I. Schmidt and J.J. Yang, Phys. Rev. **D70**, 116003 (2004).
93. K.P.O. Diener, S. Dittmaier, and W. Hollik, Phys. Rev. **D69**, 073005 (2004);
A.B. Arbuzov, D.Y. Bardin, and L.V. Kalinovskaya, JHEP **0506**, 078 (2005).
94. K.P.O. Diener, S. Dittmaier, and W. Hollik, Phys. Rev. **D72**, 093002 (2005).
95. B.A. Dobrescu and R.K. Ellis, Phys. Rev. **D69**, 114014 (2004).
96. A.D. Martin, R.G. Roberts, W.J. Stirling, and R.S. Thorne, Eur. Phys. J. **C39**, 155 (2005).
97. CHARM: J. Dorenbosch *et al.*, Z. Phys. **C41**, 567 (1989).
98. CALO: L.A. Ahrens *et al.*, Phys. Rev. **D41**, 3297 (1990).
99. CHARM II: P. Vilain *et al.*, Phys. Lett. **B335**, 246 (1994).
100. See also J. Panman, p. 504 of Ref. 4.
101. ILM: R.C. Allen *et al.*, Phys. Rev. **D47**, 11 (1993);
LSND: L.B. Auerbach *et al.*, Phys. Rev. **D63**, 112001 (2001).
102. SSF: C.Y. Prescott *et al.*, Phys. Lett. **B84**, 524 (1979);
For a review, see P. Souder, p. 599 of Ref. 4.
103. E. J. Beise, M. L. Pitt and D. T. Spayde, Prog. Part. Nucl. Phys. **54**, 289 (2005).
104. For reviews and references to earlier work, see M.A. Bouchiat and L. Pottier, Science **234**, 1203 (1986);
B.P. Masterson and C.E. Wieman, p. 545 of Ref. 4.
105. Cesium (Boulder): C.S. Wood *et al.*, Science **275**, 1759 (1997).
106. Cesium (Paris): J. Guéna, M. Lintz and M.A. Bouchiat, physics/0412017.
107. Thallium (Oxford): N.H. Edwards *et al.*, Phys. Rev. Lett. **74**, 2654 (1995);
Thallium (Seattle): P.A. Vetter *et al.*, Phys. Rev. Lett. **74**, 2658 (1995).
108. Lead (Seattle): D.M. Meekhof *et al.*, Phys. Rev. Lett. **71**, 3442 (1993).
109. Bismuth (Oxford): M.J.D. MacPherson *et al.*, Phys. Rev. Lett. **67**, 2784 (1991).
110. V.A. Dzuba, V.V. Flambaum, and O.P. Sushkov, Phys. Lett. **141A**, 147 (1989);
S.A. Blundell, J. Sapirstein, and W.R. Johnson, Phys. Rev. Lett. **65**, 1411 (1990)
and Phys. Rev. **D45**, 1602 (1992);
For reviews, see S.A. Blundell, W.R. Johnson, and J. Sapirstein, p. 577 of Ref. 4;
J.S.M. Ginges and V.V. Flambaum, Phys. Reports **397**, 63 (2004);
J. Guena, M. Lintz and M. A. Bouchiat, Mod. Phys. Lett. **A20**, 375 (2005).
111. V.A. Dzuba, V.V. Flambaum, and O.P. Sushkov, Phys. Rev. **A56**, R4357 (1997).
112. S.C. Bennett and C.E. Wieman, Phys. Rev. Lett. **82**, 2484 (1999).
113. M.A. Bouchiat and J. Guéna, J. Phys. (France) **49**, 2037 (1988).
114. A. Derevianko, Phys. Rev. Lett. **85**, 1618 (2000);
V.A. Dzuba, C. Harabati, and W.R. Johnson, Phys. Rev. **A63**, 044103 (2001);
M.G. Kozlov, S.G. Porsev, and I.I. Tupitsyn, Phys. Rev. Lett. **86**, 3260 (2001).
115. A.I. Milstein and O.P. Sushkov, Phys. Rev. **A66**, 022108 (2002);
W.R. Johnson, I. Bednyakov, and G. Soff, Phys. Rev. Lett. **87**, 233001 (2001);
V.A. Dzuba, V.V. Flambaum, and J.S. Ginges, Phys. Rev. **D66**, 076013 (2002);

- M.Y. Kuchiev and V.V. Flambaum, Phys. Rev. Lett. **89**, 283002 (2002);
 A.I. Milstein, O.P. Sushkov, and I.S. Terekhov, Phys. Rev. Lett. **89**, 283003 (2002);
 V.V. Flambaum and J.S.M. Ginges, physics/0507067.
116. J. Erler, A. Kurylov, and M.J. Ramsey-Musolf, Phys. Rev. **D68**, 016006 (2003).
117. V.A. Dzuba *et al.*, J. Phys. **B20**, 3297 (1987).
118. Ya.B. Zel'dovich, Sov. Phys. JETP **6**, 1184 (1958);
 For recent discussions, see V.V. Flambaum and D.W. Murray, Phys. Rev. **C56**, 1641 (1997);
 W.C. Haxton and C.E. Wieman, Ann. Rev. Nucl. Part. Sci. **51**, 261 (2001).
119. J.L. Rosner, Phys. Rev. **D53**, 2724 (1996).
120. S.J. Pollock, E.N. Fortson, and L. Wilets, Phys. Rev. **C46**, 2587 (1992);
 B.Q. Chen and P. Vogel, Phys. Rev. **C48**, 1392 (1993).
121. B.W. Lynn and R.G. Stuart, Nucl. Phys. **B253**, 216 (1985).
122. *Physics at LEP*, ed. J. Ellis and R. Peccei, CERN 86-02, Vol. 1.
123. PETRA: S.L. Wu, Phys. Reports **107**, 59 (1984);
 C. Kiesling, *Tests of the Standard Theory of Electroweak Interactions*, (Springer-Verlag, New York, 1988);
 R. Marshall, Z. Phys. **C43**, 607 (1989);
 Y. Mori *et al.*, Phys. Lett. **B218**, 499 (1989);
 D. Haidt, p. 203 of Ref. 4.
124. For reviews, see D. Schaile, p. 215, and A. Blondel, p. 277 of Ref. 4.
125. SLD: K. Abe *et al.*, Phys. Rev. Lett. **84**, 5945 (2000).
126. SLD: K. Abe *et al.*, Phys. Rev. Lett. **85**, 5059 (2000).
127. SLD: K. Abe *et al.*, Phys. Rev. Lett. **86**, 1162 (2001).
128. DELPHI: P. Abreu *et al.*, Z. Phys. **C67**, 1 (1995);
 OPAL: K. Ackerstaff *et al.*, Z. Phys. **C76**, 387 (1997).
129. SLD: K. Abe *et al.*, Phys. Rev. Lett. **78**, 17 (1997).
130. ALEPH, DELPHI, L3, OPAL, SLD, LEP Electroweak Working Group, SLD Electroweak and Heavy Flavour Groups: J. Alcarez *et al.*, hep-ex/0511027.
131. CDF: D. Acosta *et al.*, Phys. Rev. **D71**, 052002 (2005).
132. H1: A. Aktas *et al.*, Phys. Lett. **B632**, 35 (2006).
133. Results of difermion measurements at LEP2 can be found at URL <http://lepewwg.web.cern.ch>.
134. ALEPH, DELPHI, L3, and OPAL Collaborations, and the LEP Working Group for Higgs Boson Searches: D. Abbaneo *et al.*, Phys. Lett. **B565**, 61 (2003).
135. A. Leike, T. Riemann, and J. Rose, Phys. Lett. **B273**, 513 (1991);
 T. Riemann, Phys. Lett. **B293**, 451 (1992).
136. E158: P.L. Anthony *et al.*, Phys. Rev. Lett. **95**, 081601 (2005);
 the implications are discussed in A. Czarnecki and W.J. Marciano, Int. J. Mod. Phys. A **15**, 2365 (2000).
137. J. Erler and M.J. Ramsey-Musolf, Phys. Rev. **D72**, 073003 (2005);
 for the scale dependence of the weak mixing angle defined in a mass dependent renormalization scheme, see A. Czarnecki and W.J. Marciano, Int. J. Mod. Phys. A **15**, 2365 (2000).

46 10. Electroweak model and constraints on new physics

138. Qweak: D.S. Armstrong *et al.*, AIP Conf. Proc. **698**, 172 (2004);
the implications are discussed in Ref. 116.
139. A comprehensive report and further references can be found in K.G. Chetyrkin, J.H. Kühn, and A. Kwiatkowski, Phys. Reports **277**, 189 (1996).
140. J. Schwinger, *Particles, Sources and Fields*, Vol. II, (Addison-Wesley, New York, 1973);
K.G. Chetyrkin, A.L. Kataev, and F.V. Tkachev, Phys. Lett. **B85**, 277 (1979);
M. Dine and J. Sapiirstein, Phys. Rev. Lett. **43**, 668 (1979);
W. Celmaster, R.J. Gonsalves, Phys. Rev. Lett. **44**, 560 (1980);
S.G. Gorishnii, A.L. Kataev, and S.A. Larin, Phys. Lett. **B212**, 238 (1988);
S.G. Gorishnii, A.L. Kataev, and S.A. Larin, Phys. Lett. **B259**, 144 (1991);
L.R. Surguladze and M.A. Samuel, Phys. Rev. Lett. **66**, 560 (1991) and *ibid.* 2416(E).
141. A.L. Kataev and V.V. Starshenko, Mod. Phys. Lett. **A10**, 235 (1995).
142. W. Bernreuther and W. Wetzel, Z. Phys. **11**, 113 (1981);
W. Bernreuther and W. Wetzel, Phys. Rev. **D24**, 2724 (1982);
B.A. Kniehl, Phys. Lett. **B237**, 127 (1990);
K.G. Chetyrkin, Phys. Lett. **B307**, 169 (1993);
A.H. Hoang *et al.*, Phys. Lett. **B338**, 330 (1994);
S.A. Larin, T. van Ritbergen, and J.A.M. Vermaseren, Nucl. Phys. **B438**, 278 (1995).
143. T.H. Chang, K.J.F. Gaemers, and W.L. van Neerven, Nucl. Phys. **B202**, 407 (1980);
J. Jersak, E. Laermann, and P.M. Zerwas, Phys. Lett. **B98**, 363 (1981);
J. Jersak, E. Laermann, and P.M. Zerwas, Phys. Rev. **D25**, 1218 (1982);
S.G. Gorishnii, A.L. Kataev, and S.A. Larin, Nuovo Cimento **92**, 117 (1986);
K.G. Chetyrkin and J.H. Kühn, Phys. Lett. **B248**, 359 (1990);
K.G. Chetyrkin, J.H. Kühn, and A. Kwiatkowski, Phys. Lett. **B282**, 221 (1992);
K.G. Chetyrkin and J.H. Kühn, Phys. Lett. **B406**, 102 (1997).
144. B.A. Kniehl and J.H. Kühn, Phys. Lett. **B224**, 229 (1990);
B.A. Kniehl and J.H. Kühn, Nucl. Phys. **B329**, 547 (1990);
K.G. Chetyrkin and A. Kwiatkowski, Phys. Lett. **B305**, 285 (1993);
K.G. Chetyrkin and A. Kwiatkowski, Phys. Lett. **B319**, 307 (1993);
S.A. Larin, T. van Ritbergen, and J.A.M. Vermaseren, Phys. Lett. **B320**, 159 (1994);
K.G. Chetyrkin and O.V. Tarasov, Phys. Lett. **B327**, 114 (1994).
145. A.L. Kataev, Phys. Lett. **B287**, 209 (1992).
146. D. Albert *et al.*, Nucl. Phys. **B166**, 460 (1980);
F. Jegerlehner, Z. Phys. **C32**, 425 (1986);
A. Djouadi, J.H. Kühn, and P.M. Zerwas, Z. Phys. **C46**, 411 (1990);
A. Borrelli *et al.*, Nucl. Phys. **B333**, 357 (1990).
147. A.A. Akhundov, D.Yu. Bardin, and T. Riemann, Nucl. Phys. **B276**, 1 (1986);
W. Beenakker and W. Hollik, Z. Phys. **C40**, 141 (1988);
B.W. Lynn and R.G. Stuart, Phys. Lett. **B352**, 676 (1990);
J. Bernabeu, A. Pich, and A. Santamaria, Nucl. Phys. **B363**, 326 (1991).

148. CLEO: S. Chen *et al.*, Phys. Rev. Lett. **87**, 251807 (2001).
149. Belle: P. Koppenburg *et al.*, Phys. Rev. Lett. **93**, 061803 (2004).
150. BaBar: B. Aubert *et al.*, hep-ex/0507001;
BaBar: B. Aubert *et al.*, Phys. Rev. **D72**, 052004 (2005).
151. A.L. Kagan and M. Neubert, Eur. Phys. J. **C7**, 5 (1999).
152. A. Ali and C. Greub, Phys. Lett. **B259**, 182 (1991).
153. I. Bigi and N. Uraltsev, Int. J. Mod. Phys. A **17**, 4709 (2002).
154. A. Czarnecki and W.J. Marciano, Phys. Rev. Lett. **81**, 277 (1998).
155. J. Erler and D.M. Pierce, Nucl. Phys. **B526**, 53 (1998).
156. Y. Nir, Phys. Lett. **B221**, 184 (1989);
K. Adel and Y.P. Yao, Phys. Rev. **D49**, 4945 (1994);
C. Greub, T. Hurth, and D. Wyler, Phys. Rev. **D54**, 3350 (1996);
K.G. Chetyrkin, M. Misiak, and M. Münz, Phys. Lett. **B400**, 206 (1997);
C. Greub and T. Hurth, Phys. Rev. **D56**, 2934 (1997);
M. Ciuchini *et al.*, Nucl. Phys. **B527**, 21 (1998);
M. Ciuchini *et al.*, Nucl. Phys. **B534**, 3 (1998);
F.M. Borzumati and C. Greub, Phys. Rev. **D58**, 074004 (1998);
F.M. Borzumati and C. Greub, Phys. Rev. **D59**, 057501 (1999);
A. Strumia, Nucl. Phys. **B532**, 28 (1998).
157. F. Le Diberder and A. Pich, Phys. Lett. **B286**, 147 (1992).
158. T. van Ritbergen, J.A.M. Vermaseren, and S.A. Larin, Phys. Lett. **B400**, 379 (1997).
159. E821: H.N. Brown *et al.*, Phys. Rev. Lett. **86**, 2227 (2001);
E821: G.W. Bennett, *et al.*, Phys. Rev. Lett. **89**, 101804 (2002);
E821: G.W. Bennett *et al.*, Phys. Rev. Lett. **92**, 161802 (2004).
160. T. Kinoshita and M. Nio, Phys. Rev. **D70**, 113001 (2004).
161. S. Laporta and E. Remiddi, Phys. Lett. **B301**, 440 (1993);
S. Laporta and E. Remiddi, Phys. Lett. **B379**, 283 (1996).
162. J. Erler and M. Luo, Phys. Rev. Lett. **87**, 071804 (2001).
163. T. Kinoshita, Nucl. Phys. Proc. Suppl. **144**, 206 (2005).
164. For reviews, see V.W. Hughes and T. Kinoshita, Rev. Mod. Phys. **71**, S133 (1999);
A. Czarnecki and W.J. Marciano, Phys. Rev. **D64**, 013014 (2001);
T. Kinoshita, J. Phys. **G29**, 9 (2003);
M. Davier and W.J. Marciano, Ann. Rev. Nucl. Part. Sci. **54**, 115 (2004).
165. S.J. Brodsky and J.D. Sullivan, Phys. Rev. **D156**, 1644 (1967);
T. Burnett and M.J. Levine, Phys. Lett. **B24**, 467 (1967);
R. Jackiw and S. Weinberg, Phys. Rev. **D5**, 2473 (1972);
I. Bars and M. Yoshimura, Phys. Rev. **D6**, 374 (1972);
K. Fujikawa, B.W. Lee, and A.I. Sanda, Phys. Rev. **D6**, 2923 (1972);
G. Altarelli, N. Cabibbo, and L. Maiani, Phys. Lett. **B40**, 415 (1972);
W.A. Bardeen, R. Gastmans, and B.E. Laurup, Nucl. Phys. **B46**, 315 (1972).
166. T.V. Kukhto, E.A. Kuraev, A. Schiller, and Z.K. Silagadze, Nucl. Phys. **B371**, 567 (1992);
S. Peris, M. Perrottet, and E. de Rafael, Phys. Lett. **B355**, 523 (1995);

48 10. Electroweak model and constraints on new physics

- A. Czarnecki, B. Krause, and W.J. Marciano, Phys. Rev. **D52**, 2619 (1995);
A. Czarnecki, B. Krause, and W.J. Marciano, Phys. Rev. Lett. **76**, 3267 (1996).
167. G. Degrossi and G. Giudice, Phys. Rev. **D58**, 053007 (1998).
168. F. Matorras (DELPHI), contributed paper to the *International Europhysics Conference on High Energy Physics* (EPS 2003, Aachen).
169. V. Cirigliano, G. Ecker and H. Neufeld, JHEP **0208**, 002 (2002);
K. Maltman and C.E. Wolfe, Phys. Rev. **D73**, 013004 (2006).
170. J. Erler, Rev. Mex. Fis. **50**, 200 (2004).
171. K. Maltman, hep-ph/0504201.
172. S. Ghozzi and F. Jegerlehner, Phys. Lett. **B583**, 222 (2004).
173. K. Melnikov and A. Vainshtein, Phys. Rev. **D70**, 113006 (2004).
174. M. Knecht and A. Nyffeler, Phys. Rev. **D65**, 073034 (2002).
175. M. Hayakawa and T. Kinoshita, hep-ph/0112102;
J. Bijnens, E. Pallante and J. Prades, Nucl. Phys. **B626**, 410 (2002).
176. B. Krause, Phys. Lett. **B390**, 392 (1997).
177. J.L. Lopez, D.V. Nanopoulos, and X. Wang, Phys. Rev. **D49**, 366 (1994);
for recent reviews, see Ref. 164.
178. UA2: S. Alitti *et al.*, Phys. Lett. **B276**, 354 (1992);
CDF: T. Affolder *et al.*, Phys. Rev. **D64**, 052001 (2001);
DØ: V. M. Abazov *et al.*, Phys. Rev. **D66**, 012001 (2002).
179. CDF and DØ Collaborations: Phys. Rev. **D70**, 092008 (2004).
180. M. Grünwald, presented at the *International Europhysics Conference on High Energy Physics* (HEPP-EPS 2005, Lisbon).
181. F. James and M. Roos, Comput. Phys. Commun. **10**, 343 (1975).
182. J. Erler, J.L. Feng, and N. Polonsky, Phys. Rev. Lett. **78**, 3063 (1997).
183. D. Choudhury, T.M.P. Tait and C.E.M. Wagner, Phys. Rev. **D65**, 053002 (2002).
184. J. Erler and P. Langacker, Phys. Rev. Lett. **84**, 212 (2000).
185. DELPHI: P. Abreu *et al.*, Eur. Phys. J. **C10**, 415 (1999).
186. S. Bethke, Phys. Reports **403**, 203 (2004).
187. C. Glasman, hep-ex/0506035.
188. HPQCD and UKQCD: Q. Mason *et al.*, Phys. Rev. Lett. **95**, 052002 (2005).
189. J. Erler, Phys. Rev. **D63**, 071301 (2001).
190. P. Langacker and N. Polonsky, Phys. Rev. **D52**, 3081 (1995);
J. Bagger, K.T. Matchev, and D. Pierce, Phys. Lett. **B348**, 443 (1995).
191. M. Veltman, Nucl. Phys. **B123**, 89 (1977);
M. Chanowitz, M.A. Furman, and I. Hinchliffe, Phys. Lett. **B78**, 285 (1978).
192. P. Langacker and M. Luo, Phys. Rev. **D45**, 278 (1992) and references therein.
193. A. Denner, R.J. Guth, and J.H. Kühn, Phys. Lett. **B240**, 438 (1990).
194. S. Bertolini and A. Sirlin, Phys. Lett. **B257**, 179 (1991).
195. M. Peskin and T. Takeuchi, Phys. Rev. Lett. **65**, 964 (1990);
M. Peskin and T. Takeuchi, Phys. Rev. **D46**, 381 (1992);
M. Golden and L. Randall, Nucl. Phys. **B361**, 3 (1991).
196. D. Kennedy and P. Langacker, Phys. Rev. Lett. **65**, 2967 (1990);
D. Kennedy and P. Langacker, Phys. Rev. **D44**, 1591 (1991).

197. G. Altarelli and R. Barbieri, Phys. Lett. **B253**, 161 (1990).
198. B. Holdom and J. Terning, Phys. Lett. **B247**, 88 (1990).
199. B.W. Lynn, M.E. Peskin, and R.G. Stuart, p. 90 of Ref. 122.
200. An alternative formulation is given by K. Hagiwara *et al.*, Z. Phys. **C64**, 559 (1994) and *ibid.* **68**, 352(E) (1995);
K. Hagiwara, D. Haidt, and S. Matsumoto, Eur. Phys. J. **C2**, 95 (1998).
201. I. Maksymyk, C.P. Burgess, and D. London, Phys. Rev. **D50**, 529 (1994);
C.P. Burgess *et al.*, Phys. Lett. **B326**, 276 (1994).
202. R. Barbieri, A. Pomarol, R. Rattazzi and A. Strumia, Nucl. Phys. **B703**, 127 (2004).
203. K. Lane, hep-ph/0202255.
204. E. Gates and J. Terning, Phys. Rev. Lett. **67**, 1840 (1991);
R. Sundrum and S.D.H. Hsu, Nucl. Phys. **B391**, 127 (1993);
R. Sundrum, Nucl. Phys. **B395**, 60 (1993);
M. Luty and R. Sundrum, Phys. Rev. Lett. **70**, 529 (1993);
T. Appelquist and J. Terning, Phys. Lett. **B315**, 139 (1993);
D.D. Dietrich, F. Sannino and K. Tuominen, Phys. Rev. **D72**, 055001 (2005);
N.D. Christensen and R. Shrock, Phys. Lett. **B632**, 92 (2006);
M. Harada, M. Kurachi and K. Yamawaki, hep-ph/0509193.
205. H. Georgi, Nucl. Phys. **B363**, 301 (1991);
M.J. Dugan and L. Randall, Phys. Lett. **B264**, 154 (1991).
206. R. Barbieri *et al.*, Nucl. Phys. **B341**, 309 (1990).
207. M.E. Peskin and J.D. Wells, Phys. Rev. **D64**, 093003 (2001).
208. H.J. He, N. Polonsky, and S. Su, Phys. Rev. **D64**, 053004 (2001);
V.A. Novikov, L.B. Okun, A.N. Rozanov, and M.I. Vysotsky, Sov. Phys. JETP **76**, 127 (2002);
S. S. Bulanov, V. A. Novikov, L. B. Okun, A. N. Rozanov and M. I. Vysotsky, Yad. Fiz. **66**, 2219 (2003) and references therein.
209. For a review, see D. London, p. 951 of Ref. 4;
a recent analysis is M.B. Popovic and E.H. Simmons, Phys. Rev. **D58**, 095007 (1998);
for collider implications, see T.C. Andre and J.L. Rosner, Phys. Rev. **D69**, 035009 (2004).
210. P. Langacker, M. Luo, and A.K. Mann, Rev. Mod. Phys. **64**, 87 (1992);
M. Luo, p. 977 of Ref. 4.
211. F.S. Merritt *et al.*, p. 19 of *Particle Physics: Perspectives and Opportunities: Report of the DPF Committee on Long Term Planning*, ed. R. Peccei *et al.* (World Scientific, Singapore, 1995).
212. G. C. Cho and K. Hagiwara, Nucl. Phys. **B574**, 623 (2000);
G. Altarelli *et al.*, JHEP **0106**, 018 (2001);
A. Kurylov, M.J. Ramsey-Musolf, and S. Su, Nucl. Phys. **B667**, 321 (2003);
A. Kurylov, M.J. Ramsey-Musolf, and S. Su, Phys. Rev. **D68**, 035008 (2003);
W. de Boer and C. Sander, Phys. Lett. **B585**, 276 (2004);
S. Heinemeyer, W. Hollik and G. Weiglein, hep-ph/0412214;

50 10. Electroweak model and constraints on new physics

- J.R. Ellis, K.A. Olive, Y. Santoso, and V.C. Spanos, Phys. Rev. **D69**, 095004 (2004);
S. P. Martin, K. Tobe and J. D. Wells, Phys. Rev. **D71**, 073014 (2005);
G. Marandella, C. Schappacher and A. Strumia, Nucl. Phys. **B715**, 173 (2005).
213. C.T. Hill and E.H. Simmons, Phys. Reports **381**, 235 (2003);
R. S. Chivukula, E. H. Simmons, H. J. He, M. Kurachi and M. Tanabashi, Phys. Rev. **D70**, 075008 (2004).
214. K. Agashe, A. Delgado, M.J. May, and R. Sundrum, JHEP **0308**, 050 (2003);
M. Carena *et al.*, Phys. Rev. **D68**, 035010 (2003);
for reviews, see the articles on “Extra Dimensions” in this *Review* and I. Antoniadis, hep-th/0102202.
215. For a review, see M. Perelstein, hep-ph/0512128.
216. G. Altarelli, R. Barbieri, and S. Jadach, Nucl. Phys. **B369**, 3 (1992) and **B376**, 444(E) (1992).
217. A. De Rújula *et al.*, Nucl. Phys. **B384**, 3 (1992).
218. K. Hagiwara *et al.*, Phys. Rev. **D48**, 2182 (1993).
219. C.P. Burgess and D. London, Phys. Rev. **D48**, 4337 (1993).
220. For a review, see A. Leike, Phys. Reports **317**, 143 (1999).
221. M. Cvetič and P. Langacker, Phys. Rev. **D54**, 3570 (1996).
222. R.S. Chivukula and E.H. Simmons, Phys. Rev. **D66**, 015006 (2002).
223. S. Chaudhuri *et al.*, Nucl. Phys. **B456**, 89 (1995);
G. Cleaver *et al.*, Phys. Rev. **D59**, 055005 (1999).
224. M. Carena, A. Daleo, B. A. Dobrescu and T. M. P. Tait, Phys. Rev. **D70**, 093009 (2004).
225. CDF: F. Abe *et al.*, Phys. Rev. Lett. **79**, 2192 (1997);
A. Abulencia *et al.*, Phys. Rev. Lett. **95**, 252001 (2005);
preliminary CDF and D0 limits from Run II may be found at URLs <http://www-cdf.fnal.gov/> and <http://www-d0.fnal.gov/>.
226. J. Kang and P. Langacker, Phys. Rev. **D71**, 035014 (2005).
227. J. Erler and P. Langacker, Phys. Lett. **B456**, 68 (1999).
228. T. Appelquist, B.A. Dobrescu, and A.R. Hopper, Phys. Rev. **D68**, 035012 (2003);
R.S. Chivukula, H.J. He, J. Howard, and E.H. Simmons, Phys. Rev. **D69**, 015009 (2004).
229. P. Langacker and M. Plümacher, Phys. Rev. **D62**, 013006 (2000).
230. R. Casalbuoni, S. De Curtis, D. Dominici, and R. Gatto, Phys. Lett. **B460**, 135 (1999);
J.L. Rosner, Phys. Rev. **D61**, 016006 (2000).